

1
2 **Norwegian Sea Oceanic Basin and Prograded Margins**
3 **Composite Tectono-Sedimentary Element**
4

5 Faleide, J.I.¹, Abdelmalak, M.M.¹, Zastrozhnov, D.¹, Lasabuda, A.P.E¹,
6 Hjelstuen, B.O.², Laberg, J.S.³, Planke, S.^{1,4}
7

8 ¹Department of Geosciences, University of Oslo, Oslo, Norway

9 ²Department of Earth Science, University of Bergen, Bergen, Norway

10 ³Department of Geosciences, UiT The Arctic University of Norway, Tromsø, Norway

11 ⁴Volcanic Basin Energy Research (VBER), Oslo, Norway
12
13

14 Corresponding author: Jan Inge Faleide, j.i.faleide@geo.uio.no
15
16

17 **Abstract**

18 The Norwegian Sea oceanic basins and prograded margins developed since NE Atlantic
19 breakup in the earliest Eocene. Significant amounts of sediments were fed to the regionally
20 subsiding and widening Norwegian Sea during the Cenozoic as a result of several phases of
21 uplift and erosion of the bounding shelves and their hinterland. Despite an overall passive
22 margin evolution, the area experienced tectonic events and associated processes that
23 interrupted the regional subsidence causing contraction/inversion and tilting. The post-
24 breakup depositional history of the mid-Norwegian margin comprises two main stages: (1)
25 middle Eocene-Pliocene margin subsidence and relatively modest sedimentation during a
26 period of climatic decline; and (2) latest Pliocene-Pleistocene full-scale Northern Hemisphere
27 glaciations resulting in deep erosion of shelves and hinterlands, and very high sedimentation
28 rates and large-scale continental margin progradation. Slope failures within rapidly deposited
29 glacial sediments affected both prograded margins releasing large slides travelling down-
30 slope into the oceanic Norway and Lofoten basins. Despite a long exploration history for
31 prospects in deeper waters and large amounts of data acquisition, no significant discovery has
32 been made.
33
34

35 **Introduction** (no heading)

36

37 The present paper reviews the geology of the Norwegian Sea Oceanic Basin and Prograded
38 Margins Composite Tectono-Sedimentary Element (NSOBPM CTSE; Fig. 1), which has
39 developed since NE Atlantic breakup in the earliest Eocene (e.g. [Brekke 2000](#); [Eldholm et al.](#)
40 [2002](#); [Faleide et al. 2008](#)). The mid-Norwegian (62-69°N) and western Barents Sea-Svalbard
41 (69-78°N) continental margins (Fig. 1) experienced regional subsidence in response to
42 thermal cooling and sediment loading during the Cenozoic widening and deepening of the
43 Norwegian-Greenland Sea. Significant amounts of sediments were fed to the Norwegian Sea
44 during the Cenozoic post-breakup stage as a result of several phases of uplift and erosion of
45 the bounding shelves and their hinterland. The sedimentary record of the prograded margin
46 provides the best age constraints on the Cenozoic exhumation of the adjacent areas (e.g.
47 [Vorren et al. 1991](#); [Richardson et al. 1991](#); [Faleide et al. 1996](#); [Hjelstuen et al. 1996, 1999](#);
48 [Stuevold and Eldholm 1996](#); [Laberg et al. 2005a](#); [Henriksen et al. 2011](#); [Baig et al. 2016](#);
49 [Ktenas et al. 2017, 2019, 2023](#); [Lasabuda et al. 2021](#); [Eidvin et al. 2022](#)). In addition,
50 sediment input by ocean currents contributed ([Rebesco et al. 2014](#); [Rydningen et al. 2020](#);
51 [Bjordal-Olsen et al. 2023](#)). Despite an overall passive margin evolution, the area experienced
52 tectonic events and associated processes that interrupted the regional subsidence causing
53 contraction/inversion and tilting (e.g. [Doré and Lundin 1996](#); [Lundin and Doré 2002](#); [Mosar](#)
54 [et al. 2002](#); [Praeg et al. 2005](#); [Stoker et al. 2005a](#)).

55

56 The post-breakup depositional history of the mid-Norwegian margin (Møre-Vøring margins;
57 Fig. 1B) comprises two main stages (e.g. [Vorren et al. 1998](#); [Hjelstuen et al. 1999](#); [Laberg et](#)
58 [al. 2005a](#); [Stoker et al. 2005b,c](#)): (1) middle Eocene-Pliocene margin subsidence and variable
59 sedimentation rates during a period of climatic decline from greenhouse towards icehouse
60 conditions; and (2) latest Pliocene-Pleistocene Northern Hemisphere glaciations resulting in
61 deep continental erosion, very high sedimentation rates and large-scale glacial sedimentary
62 fan construction, and continued margin subsidence and progradation ([Dahlgren et al. 2005](#)).
63 In Eocene to early Pliocene times, the Møre and Vøring margins (Fig. 1B) were located in a
64 distal position relative to sediment supply from Scandinavia, and biogenic ooze makes up a
65 significant part of the succession. Clay-rich sediments were deposited on more proximal parts
66 of the mid-Norwegian margin in this period ([Laberg et al. 2005b](#); [Eidvin et al. 2022](#)). The
67 margin setting was changed at the Pliocene-Pleistocene transition (~2.7 Ma) when the
68 Northern Hemisphere glaciations led to rapid progradation gradually forming a huge, regional

69 depocentre near the shelf edge along the entire Vøring margin (Rise *et al.* 2005; Ottesen *et al.*
70 2009, 2012; Bjordal-Olsen *et al.* 2023) and the North Sea Trough Mouth Fan (TMF) at the
71 northern North Sea-Møre margin (King *et al.* 1996; Nygård *et al.* 2005; Batchelor *et al.*
72 2017).

73

74 Along the western Barents Sea-Svalbard margin (Fig. 1B) the passive margin evolution
75 started later due to ongoing basin formation/development on the shear margin during Eocene-
76 ?Oligocene time (Faleide *et al.* 2024b). Major margin progradation occurred in response to
77 regional uplift and glacial erosion of the Barents Sea shelf during latest Pliocene-Pleistocene
78 time (Faleide *et al.* 1996; Hjelstuen *et al.* 1996; Solheim *et al.* 1998; Vorren *et al.* 1998;
79 Henriksen *et al.* 2011). The links between uplift/erosion of the shelf and deposition in the
80 prograded margin offer a unique source-to-sink system where mass balance can be carried
81 out (e.g. Dimakis *et al.* 1998; Lasabuda *et al.* 2021; Medvedev *et al.* 2022). Glacial erosion
82 by ice streams shaped the Barents Sea shelf and large sediment volumes were transported to
83 the margin and deposited as km-thick trough mouth fans (Faleide *et al.* 1996; Hjelstuen *et al.*
84 1996; Solheim *et al.* 1998; Vorren *et al.* 1998; Andreassen *et al.* 2004; Andreassen and
85 Winsborrow 2009; Laberg *et al.* 2010).

86

87 Slope failure within rapidly deposited glacial sediments affected both prograded margins
88 releasing large slides travelling down-slope into the oceanic Norway and Lofoten basins
89 (Laberg and Vorren 1993, 2000; Laberg *et al.* 2002; Haflidason *et al.* 2004; Bryn *et al.* 2005;
90 Evans *et al.* 2005; Hjelstuen *et al.* 2005, 2007; Kvalstad *et al.* 2005a,b; Riis *et al.* 2005;
91 Solheim *et al.* 2005; Rise *et al.* 2006).

92

93

94 **Age**

95

96 The Norwegian Sea Oceanic Basin and Prograded Margins CTSE (NSOBPM CTSE)
97 comprises strata of Eocene to recent age deposited since continental breakup and onset of
98 seafloor spreading in the earliest Eocene.

99

100

101 **Geographic location and dimensions**

102

103 The NSOBPM CTSE comprises most of the continental margin between 62° and 80°N (Fig.
104 1) covering an area of approximately 745 000 km². On the mid-Norwegian margin (62-
105 69°N), it covers the underlying pre-breakup CTSE's (Bunkholt *et al.* 2021; Tsikalas *et al.*
106 2022; Faleide *et al.* 2024a) and extends further into the oceanic domain (Figs. 1 and 2).
107 Along the western Barents Sea-Svalbard margin (69-78°N), it covers the marginal basins of
108 the West Barents Shear Margin CTSE (Faleide *et al.* 2024b).

109
110

111 **Principal data sets**

112

113 The principal data sets comprise exploration wells and scientific boreholes tied to 2D/3D
114 seismic reflection data (Fig. 3).

115

116 *Wells*

117

118 More than 400 exploration wells have been completed within the NSOBPM CTSE area
119 (Norwegian Offshore Directorate FactPages; <https://factpages.sodir.no/en>), most of them in
120 proximal parts of the Vøring margin (Fig. 3A) where they also reach the underlying CTSE
121 (Bunkholt *et al.* 2021). In the SW Barents Sea, only 11 wells cover the prograded margin. In
122 the exploration wells the shallowest stratigraphy is seldom sampled since most of them are
123 drilled with a return to seabed for the upper part. Key wells used for definition of the main
124 Cenozoic lithostratigraphic units are highlighted and labelled in Figure 3 (see description of
125 these units below). Scientific (DSDP, ODP, IODP; Talwani *et al.* 1976; Eldholm *et al.* 1989;
126 Planke *et al.* 2023) and shallow stratigraphic boreholes (e.g. Rise and Sættem 1994; Sættem
127 *et al.* 1994; Grogan *et al.* 1998) provide continuous cores of the shallow stratigraphy, in
128 particular at the outer margin (Fig. 3A).

129

130 *Seismic data*

131

132 The mid-Norwegian margin is extensively covered by a dense grid of 2D seismic lines
133 complemented by 3D seismic in large parts (Fig. 3B). For regional mapping the main 2D data
134 set is the reprocessed CFI_MNR (Mid Norway Renaissance) survey by TGS. The outer
135 margin is covered by several extensive 3D cubes (Atlantic Margin North/South) and these

136 were used to identify drilling targets for the recent IODP Expedition 396 (Planke *et al.* 2023).
137 In the SW Barents Sea, proximal parts of the prograded margin is also covered by a dense
138 grid of 2D seismic lines and a few 3D seismic cubes. Here, the CFI-NBR (Norwegian
139 Barents Sea Renaissance) of TGS is the most important 2D set, while SWB17 and Carlsen
140 represent extensive 3D cubes. The 2D and 3D seismic datasets mentioned above are all of
141 very good quality contributing to consistent and well-constrained regional mapping results.
142 However, in the oceanic parts, the seismic data coverage is generally poor (Fig. 3B).
143 Important 2D data sets covering the outer margin and the oceanic Norway and Lofoten basins
144 (NPD-HB-96, NPD-HV-96, NPD-LOS-99) were acquired by Norwegian authorities in
145 relation to the United Nations Convention on the Law of the Sea (UNCLOS) to support
146 Norway's claims with respect to an extended continental shelf into the Norwegian Sea.

147

148 *Other data*

149

150 Complementary data include bathymetry (IBCAO 4.0; Jakobsson *et al.* 2020), gravity
151 (Skilbrei *et al.* 2000; Olesen *et al.* 2010) and magnetic (Verhoef *et al.* 1996; Maus *et al.*
152 2009; Olesen *et al.* 2010; Nasuti and Olesen 2014) data. Heat flow data are generally sparse
153 (Fig. 3A) but some exist that will be discussed in a later section.

154

155

156 **Tectonic setting, TSE boundaries, and main tectonic /erosional/ depositional phases**

157

158 *Tectonic setting and boundaries*

159

160 The NSOBPM CTSE developed in response to the final breakup and subsequent sea floor
161 spreading in the Norwegian-Greenland Sea since the earliest Eocene (Fig. 4; e.g. Eldholm *et al.*
162 2002; Faleide *et al.* 2008; Gaina *et al.* 2009). The mid-Norwegian rifted margin can be
163 subdivided into three segments (Møre, Vøring and Lofoten-Vesterålen; Fig. 1) having
164 different margin architectures that reflect different styles of margin progradation. The western
165 Barents Sea-Svalbard shear margin bounds a broad shelf area in the Barents Sea that sourced
166 widespread margin progradation.

167

168 The outline of the CTSE is shown in Figure 1B. The eastern (landward) extent is defined by
169 the subcrop of the near base Eocene at the seabed close to the coast. Towards west, the

170 Eocene and younger sedimentary succession belonging to the NSOBPM CTSE extends into
171 and cover oceanic crust in the Norwegian-Greenland Sea. The Norway Basin opened during
172 Eocene before the Ægir Ridge became extinct (Breivik *et al.* 2006, 2012) and spreading
173 moved to the Kolbeinsey Ridge (west of the Jan Mayen Microcontinent; Fig. 1A). The
174 prograded margin associated with the North Sea TMF (King *et al.* 1996; Nygård *et al.* 2005;
175 Batchelor *et al.* 2017) reached parts of the Norway Basin east of the Ægir Ridge (Hjelstuen
176 and Andreassen 2015; Hjelstuen and Sejrup 2021). The CTSE boundary is drawn at the
177 mouth of the Norwegian Channel that sourced this fan (Fig. 1B).

178

179 In the Lofoten Basin, formed by seafloor spreading along the Mohns Ridge (Fig. 1B), most of
180 the CTSE belong to the Bjørnøya TMF that was sourced from the Barents Sea shelf (Fiedler
181 and Faleide 1996; Faleide *et al.* 1996; Hjelstuen and Sejrup 2021). To the north, the
182 Storfjorden TMF occupies the area between the Barents Sea shelf and the Knipovich Ridge
183 (Faleide *et al.* 1996; Hjelstuen *et al.* 1996; Lasabuda *et al.* 2018a). The CTSE narrows further
184 northwards (Fig. 1B) and is filled with minor fans outside fjords in western Svalbard
185 (Spitsbergen) (Solheim *et al.* 1998; Forsberg *et al.* 1999; Butt *et al.* 2000a,b).

186

187 The boundary between the Prograded Margin and Oceanic Basin TSE's reflects a facies
188 transition zone separating dominantly prograding sediments (delivered from the continents)
189 and dominantly aggrading sediments in the deep oceanic basin. However, it is difficult to
190 delineate this as a distinct boundary since the two facies interfinger in distal parts of the
191 prograded margin. Furthermore, the data coverage is generally poor in deeper parts of the
192 oceanic basin. The distal boundary of the Prograded Margin TSE (Fig. 1B) is guided by the
193 thickness distribution within the huge sedimentary fans reflecting major outbuilding of
194 sediments into the oceanic basins.

195

196 *Main tectonic, erosional and depositional phases*

197

198 Breakup occurred in the earliest Eocene (Fig. 4) and was associated with massive magmatism
199 within the North Atlantic Igneous Province (Skogseid *et al.* 2000; Eldholm *et al.* 2002;
200 Faleide *et al.* 2008; Planke *et al.* 2023). Initial spreading occurred subaerially forming the
201 Møre and Vøring marginal highs covered by thick piles of lava flows (Fig. 2; Planke *et al.*
202 2000, 2017; Berndt *et al.* 2001; Abdelmalak *et al.* 2016). Regional Eocene-Oligocene

203 subsidence by cooling and sediment loading caused burial of the marginal highs so that the
204 margin could prograde further into the Norwegian Sea oceanic basins.

205

206 The passive margin development started later along the western Barents Sea margin (Faleide
207 *et al.* 2024b). Here, Eocene-Oligocene basins formed in a shear-dominated setting before
208 passive margin development was established in Oligocene-Miocene time when the Barents
209 Sea shelf was source area for sediments building out westwards.

210

211 Mid-Cenozoic compressional deformation including domes/anticlines, reverse faults, and
212 broad-scale inversion is well documented on the Vøring margin (Fig. 2), but its timing and
213 significance are debated (Doré and Lundin 1996; Vågnes *et al.* 1998; Lundin and Doré, 2002;
214 Løseth and Henriksen, 2005; Stoker *et al.* 2005a; Doré *et al.* 2008; Lundin *et al.* 2013). The
215 main phase of deformation is likely Miocene in age but some of the structures were
216 apparently initiated earlier in late Eocene–Oligocene times. A multi-phase growth history is
217 suggested for the domes based on seismic onlap patterns (Fig. 2): late Eocene-early
218 Oligocene for the Ormen Lange Dome, late Eocene-early Miocene for the Helland Hansen
219 Arch, and Early-Middle Miocene for the Naglfar Dome by Doré *et al.* (1999), whereas
220 Hjelstuen *et al.* (1997) suggested a Late Oligocene-Miocene age for both Vema and Naglfar
221 domes. On the other hand, Vågnes *et al.* (1998) reported a surprisingly constant growth rate
222 for the Ormen Lange Dome from Eocene to present, while Lundin and Doré (2002)
223 documented episodic activity. Miocene compression is also recorded on the western Barents
224 Sea margin (Richardson *et al.* 1991; Gac *et al.* 2016; Gabrielsen *et al.* 2023).

225

226 There is increasing evidence on the mid-Norwegian margin for late Miocene outbuilding on
227 the inner shelf (Molo Formation; Eidvin *et al.* 2007) indicating a regional, moderate uplift of
228 Fennoscandia (e.g. Eidvin *et al.* 2000, 2007; Faleide *et al.* 2002; Løseth and Henriksen, 2005;
229 Lidmar-Bergström *et al.* 2007). Pre-glacial uplift also affected the NW Barents Sea shelf
230 including Svalbard and a late Miocene age is indicated by observed tilting of the Vestbakken
231 Volcanic Province (Fig. 2; Jebsen and Faleide 1998). A late Miocene exhumation event is
232 also reported based on apatite fission track analysis (AFTA) of samples from several wells in
233 the Barents Sea (Green and Duddy 2010).

234

235 The Miocene succession preserves a record of deep-water sedimentation that indicates an
236 expansion of contourite sediment drifts (Fig. 2; Eiken and Hinz, 1993; Laberg *et al.*, 2005a,b;
237 Stoker *et al.*, 2005b; Rebesco *et al.* 2014; Rydningen *et al.* 2020; Bjordal-Olsen *et al.* 2023).

238

239 A marked shift in prograding style occurred when latest Pliocene-Pleistocene glacial
240 sediments prograded westward as continental ice sheets expanded onto the shelf (Henriksen
241 *et al.* 2005; Hjelstuen and Sejrup 2021; Lien *et al.* 2022). Large Pleistocene depocenters
242 formed fans in front of bathymetric troughs sourced by ice streams eroding the shelf
243 (Faleide *et al.* 1996; Laberg and Vorren 1996; Vorren *et al.* 1989; Sejrup *et al.* 2003;
244 Andreassen *et al.* 2004; Dahlgren *et al.* 2005; Nygård *et al.* 2005; Ottesen *et al.* 2002, 2005;
245 Rise *et al.* 2005; Andreassen and Winsborrow 2009; Patton *et al.* 2022). Pleistocene uplift
246 and glacial erosion of the Barents Sea shelf and deposition of large volumes of glacial
247 deposits in submarine fans along the margin resulted in a regional tilt of the margin (Dimakis
248 *et al.* 1998). In terms of post-opening sediments, the glacial component constitutes more than
249 half of the total volume deposited on the mid-Norwegian and western Barents Sea margins
250 (Lasabuda *et al.* 2021). The greatly enhanced Pleistocene deposition rates within the fans
251 induced excess pore pressure and sediment instability resulting in a series of submarine slides
252 of various sizes and timing (Kuvaas and Kristoffersen 1996; Hafliðason *et al.* 2004; Bryn *et*
253 *al.* 2005; Evans *et al.* 2005; Solheim *et al.* 2005; Hjelstuen *et al.* 2005, 2007; Rise *et al.* 2006;
254 Safronova *et al.* 2017; Rydningen *et al.* 2020).

255

256

257 **Underlying and overlying rock assemblages**

258

259 *Age of youngest underlying sedimentary unit*

260

261 On the mid-Norwegian margin, the youngest underlying sedimentary unit is of late Paleocene
262 (-earliest Eocene?) age represented by the Tare Fm containing tuff related to volcanic activity
263 during breakup. On the western Barents Sea margin, the youngest sedimentary unit
264 underlying the prograded margin TSE is of Oligocene-Miocene age (Fig. 4).

265

266 *Age of oldest overlying sedimentary unit*

267

268 The NSOBPM CTSE comprises sedimentary strata from Eocene to recent sediments at the
269 present seafloor.

270

271

272 **Subdivision and internal structure**

273

274 The overall prograded margin TSE can be subdivided into three main systems (Fig. 1): (1)
275 Northern North Sea-Møre Margin, (2) Vøring Margin and (3) Western Barents Sea margin.
276 For the Møre and Vøring margins there are a lower part bounded by the Møre and Vøring
277 marginal highs respectively, which represented restrictions to Eocene-Oligocene margin
278 progradation (Fig. 5). Eocene-Oligocene depocenters are located landward of the escarpments
279 bounding the marginal highs (Fig. 6A). The marginal highs were gradually buried and the
280 Neogene units were able to prograde farther out into the oceanic basin in the Norwegian Sea.

281

282 A variety of mechanisms have been suggested for the initiation and growth of the
283 compressional structures which are widespread in the Vøring Basin and the adjacent Jan
284 Mayen Corridor (Fig. 2). These include (1) plate-driving forces (ridge push, slab pull, mantle
285 drag), (2) differences in spreading rates, (3) asymmetric spreading, (4) changes in absolute
286 plate motion, (5) far-field transmission of orogenic stress, (6) reactivation of basement
287 structures/lineaments, and (7) differential sedimentary loading and compaction. Several of
288 these mechanisms have likely interacted during the complex evolution of the structures (see
289 discussion in [Mosar et al. 2002](#) and [Doré et al. 2008](#)). The distinct compressional episode in
290 the middle Miocene causing major growth of many dome structures, coincided in time with
291 the formation of Iceland and its surrounding pedestal and body forces related to this elevated
292 bathymetry/topography may have increased the compressional stresses affecting the dome
293 structures ([Doré et al. 2008](#)). It also coincides with an increase in spreading rate and a change
294 in absolute plate motion ([Mosar et al. 2002](#)). The relief of many domes was amplified by
295 differential loading and compaction during margin progradation. The most prominent domes
296 are the *Helland-Hansen Arch*, *Modgun Arch*, *Vema Dome* and *Naglfar Dome* (Figs. 2 and 5).
297 The mid-Cenozoic domes also formed temporary barriers to progradation, in particular during
298 the Miocene when the compressional deformation was strongest. In contrast, within the
299 central and southern Møre Basin compressional structures are less common (Fig. 2), which
300 could be the result of strain partitioning along the Jan Mayen Fracture Zone ([Doré et al.](#)
301 [2008](#)).

302
303
304
305
306
307
308
309
310
311
312
313
314
315
316
317
318
319
320
321
322
323
324
325
326
327
328
329
330
331
332
333
334
335

The main prograding units on the mid-Norwegian margin are associated with the North Sea TMF on the northern North Sea-Møre Margin and the Naust depocenter on the outer shelf of the Vøring Margin (Figs. 5 and 6B). The North Sea TMF is located at the mouth of the Norwegian Channel and was fed by the ice stream shaping the channel, which was linked to the Scandinavian ice sheet (King *et al.* 1996; Sejrup *et al.* 2003). The fan is divided into two provinces by the Møre Marginal High (Fig. 5A,B; Nygård *et al.* 2005). On the seaward side of the high the data coverage is sparse and the stratigraphy is poorly constrained in the Norway Basin (see profiles A and B in Fig. 5).

The northern North Sea-Møre margin comprises several slides related to slope failure (Fig. 7). The most recent and exposed slide is the prominent Storegga Slide, which was studied in large detail in relation to development of the Ormen Lange Field that is located in the scar of the slide (Haflidason *et al.* 2004; Berg *et al.* 2005; Bryn *et al.* 2005; Kvalstad *et al.* 2005a,b; Solheim *et al.* 2005). The Storegga Slide occurred 8200 years ago (Haflidason *et al.* 2005) soon after the last deglaciation of the Norwegian margin. Rapid loading from glacial deposits generated excess pore pressure and reduced the effective shear strength of the underlying clays and oozes. Failure and sliding of the unstable sediments were likely triggered by a strong earthquake located downslope from Ormen Lange (Haflidason *et al.* 2004; Bryn *et al.* 2005). Similar mechanisms were likely involved in earlier slide events on the northern North Sea-Møre margin during the last ~1.1 m.y. Three mass transport deposits are identified corresponding to the Tampen (~130 ka), Møre (~300 ka) and Stad (~400 ka) slides (Nygård *et al.* 2005; Hjelstuen and Grinde 2016). The Pleistocene depocenter on the outer shelf of the Vøring margin comprises prograding wedges of glacial sediments belonging to the Naust Fm (Fig. 5C-E; Rise *et al.* 2005; Ottesen *et al.* 2009, 2012; Bjordal-Olsen *et al.* 2023). A system of craters and mounds are found at the base of the glacially influenced sediments along the mid-Norwegian margin. Rapid sedimentation by low-permeable glacial muds caused overpressure in oozes, which were remobilized from the evacuation craters into the associated mounds (Riis *et al.* 2005; Bellwald *et al.* 2024).

The western Barents Sea prograded margin can be further subdivided into a series of trough mouth fans (TMFs) that developed in front of cross-shelf troughs formed by glacial erosion, mainly by ice streams (e.g. Faleide *et al.* 1996; Sejrup *et al.* 2003; Laberg *et al.* 2010, 2012; Alexandropoulou *et al.* 2021; Hjelstuen and Sejrup 2021; Patton *et al.* 2022). The Bjørnøya

336 TMF is the largest when considering areal extent, and cover most of the oceanic Lofoten
337 Basin (Figs. 6B and 8A-C). The Storfjorden TMF is smaller in areal extent but has the
338 thickest sedimentary succession (Figs. 6B and 8D; Hjelstuen *et al.* 1996; Lasabuda *et al.*
339 2018a). To the north, several smaller fans are found outside fjords of western Svalbard
340 (Spitsbergen) (Fig. 8E; Solheim *et al.* 1998; Forsberg *et al.* 1999; Butt *et al.* 2000a,b). On the
341 Bjørnøya TMF, several buried megaslides 1.0 to 0.2 Ma old have been identified (Figs. 7 and
342 8C). The two largest of these involved one order of magnitude more sediment than the
343 Storegga Slide (Hjelstuen *et al.* 2007). Megaslides have also been identified on the
344 Storfjorden TMF within the lowermost glacial unit GI (Figs. 7 and 8D; Safronova *et al.*
345 2017).

346

347

348 **Sedimentary fill**

349

350 *Total thickness*

351

352 The total sedimentary thickness from seabed to the top Paleocene typically ranges between 3-
353 6 km within the prograded margins, thinning westwards into the oceanic basin (Figs. 5, 6 and
354 8).

355

356 *Stratigraphy (lithostratigraphy, seismic stratigraphy)*

357

358 The lithostratigraphy was originally defined by Dalland *et al.* (1988) for the mid-Norwegian
359 shelf (Haltenbanken at inner part of the Vøring margin). In a recent paper, Eidvin *et al.*
360 (2022) made some revisions/updates. The Cenozoic succession making up the prograded
361 margin TSE comprises four formations (from oldest to youngest): Brygge, Kai, Molo and
362 Naust (Fig. 4).

363

364 The *Brygge Formation* is of early Eocene to early Miocene age (Fig. 4). At Haltenbanken
365 (e.g. in type well 6407/1-3; Fig. 3A), it consists of mainly claystone with stringers of
366 sandstone, siltstone, limestone and marl (Dalland *et al.* 1988; Eidvin *et al.* 2022). Westwards,
367 in the Vøring and Møre basins, siliceous ooze becomes common (Dalland *et al.* 1988;
368 Bellwald *et al.* 2024).

369

370 The *Kai Formation* of middle Miocene to early Pliocene age (Fig. 4) is dominated by ooze-
371 rich claystones alternating with siltstone and sandstone in some areas. Limestone stringers,
372 glauconite and pyrite are also recorded (Dalland *et al.* 1988; Eidvin *et al.* 2022). Key wells
373 for the Kai Formation include 6407/1-2, 6507/5-1, 6609/11-1, 6508/5-1, 6507/12-1 and
374 6305/5-1 (Fig. 3A). After deposition of the ooze-rich, stratified sediments, Opal A-CT
375 conversion, polygonal faulting and fluid-flow processes have altered the sediments (Chand *et*
376 *al.* 2011; Millett *et al.* 2022).

377

378 The *Molo Formation* (type well 6407/9-5; Fig. 3A) represents a set of steep clinoforms
379 extending about 500 km from the coast off Møre to Lofoten. In proximal parts (e.g. wells
380 6610/3-1 and 6510/2-1; Fig. 3A), the unit consists of sand and some pebbles, while in more
381 distal parts it contains sand, silt and clay (Eidvin *et al.* 2022). It has been challenging to date
382 the formation and its age has been discussed extensively. According to Løseth and Henriksen
383 (2005) and Løseth *et al.* (2017) the Molo Formation is of early Pliocene age making it
384 younger than the Kai Formation (Fig. 4). Recent dating efforts (well 6610/3-1; Fig. 3A) gave
385 a late Miocene to early Pliocene age (Grøsfjeld *et al.* 2019; Dybkjær *et al.* 2021) supporting
386 the view of Eidvin *et al.* (2007, 2014, 2019) based on studies of ditch cuttings samples in
387 wells 6407/9-5, 6407/9-2 and 6407/9-1 (Fig. 3A) that the southern part of the Molo Fm
388 corresponds to the middle/upper part of the Kai Fm.

389

390 The *Naust Formation* is of latest Pliocene-Pleistocene age (< 2.75 Ma; Eidvin *et al.* 2020,
391 2022) (Fig. 4), and consists of interbedded claystone, siltstone and sand, occasionally with
392 very coarse clastics in the upper part. On the mid-Norwegian margin the type and reference
393 sections for the Naust Formation come from wells 6507/12-1 and 6507/5-1 (Fig. 3A)
394 respectively.

395

396 A formal lithostratigraphy has not been established for the western Barents Sea margin but
397 Eidvin *et al.* (2022) introduced a lithostratigraphic scheme for parts of the margin (Fig. 4).
398 The Naust Formation is extended into the SW Barents Sea with a type section in well 7117/9-
399 1 (Fig. 3A). Below they defined the new Tiskjegg Formation of Miocene age (Fig. 4) based
400 on a type section in well 7216/11-1 S (Fig. 3A). Within the underlying Torsk Formation of
401 Eocene-Oligocene age (Fig. 4) Eidvin *et al.* (2022) defined the middle Eocene Tobis Member
402 consisting of sandy fan deposits penetrated in wells 7216/11-1 S and 7316/5-1 (Fig. 3A;
403 Ryseth *et al.* 2003).

404

405 Regionally along the western Sea margin we mainly build on a well-established seismic
406 stratigraphy (Fig. 4) first presented by [Faleide et al. \(1996\)](#). They subdivided the post-
407 breakup sedimentary succession of the prograded margin into four units. G0 represents pre-
408 glacial sediments that were further subdivided into four sub-units Te1-4 and tentative ages
409 were assigned based on the age of the oceanic basement where they pinch out ([Fiedler and](#)
410 [Faleide 1996](#)). Seven seismic reflectors (R1-R7) were interpreted in the glacial sediments and
411 these formed the basis for identifying three units; GI (R7-R5), GII (R5-R1) and GIII (R1-
412 seabed) (Fig. 4). The boundaries of these units were tied to exploration wells 7117/9-1 and
413 7117/9-2 (Fig. 3A) at the Senja Ridge in the SW Barents Sea showing that they were of
414 glacial origin and of late Pliocene-Pleistocene age ([Eidvin et al. 1993](#)). R1-R7 were
415 interpreted/correlated along the entire margin and tied to DSDP Site 344, drilled at the flank
416 of the Knipovich Ridge (Fig. 3A). Later drilling at ODP Site 986 in a similar setting farther
417 north (Fig. 3A) largely confirmed the stratigraphic framework of [Faleide et al. \(1996\)](#)
418 ([Forsberg et al. 1999](#); [Butt et al. 2000b](#)). Following reanalyzes of ODP Site 986 the age of
419 R7, corresponding to the base of the glacial sediments, was changed from 2.3 to 2.7 Ma
420 ([Knies et al. 2009](#); [Alexandropoulou et al. 2021](#)).

421

422 *Depositional environment and provenance*

423

424 The Cenozoic NE Atlantic-Arctic plate tectonic evolution had large impact on the
425 paleoceanography and sedimentation in the Norwegian-Greenland Sea and its continental
426 margins (e.g. [Thiede et al. 1989](#); [Eldholm et al. 1994, 2002](#)). Ocean basin segmentation
427 caused by offsets in the initial plate boundary, local migration of the mid-ocean ridge axis
428 and changes in relative plate motion created along-margin barriers affecting watermass
429 circulation and depositional processes. The most important of such barriers were the
430 Greenland-Iceland-Faroe Ridge bounding the Norwegian-Greenland Sea towards south, and
431 the Fram Strait Gateway between the NE Atlantic and Arctic Eurasia Basin (Fig. 1A; [Laberg](#)
432 [et al. 2005a](#); [Jakobsson et al. 2007](#); [Engen et al. 2008](#); [Parnell-Turner et al. 2015](#); [Straume et](#)
433 [al. 2020](#)). Across-margin barriers also existed, in particular in the Paleogene. Regional uplift
434 along the initial plate boundary and the subsequent formation of emerged marginal highs like
435 the Møre and Vøring marginal highs (Fig. 5) had large impact on depositional processes
436 during progradation of the mid-Norwegian margin.

437

438 The early Eocene to early Miocene sediments of the Brygge Formation on the mid-
439 Norwegian (Møre-Vøring) margin are marine, mainly deposited in deep water in a distal
440 environment (Dalland *et al.* 1988). During much of the Eocene-Oligocene the Møre and
441 Vøring marginal highs were emerged and acted as sediment source area, and hindered margin
442 progradation into the developing Norwegian Sea oceanic basin. The oceanic Lofoten Basin
443 was mainly filled from the Barents Sea shelf (Fiedler and Faleide 1996; Faleide *et al.* 1996),
444 but sediments were also routed through a number of canyons along the Lofoten-Vesterålen
445 margin (Rise *et al.* 2013).

446

447 The middle Miocene to early Pliocene marine sediments of the Kai Formation were deposited
448 on the outer and middle parts of the mid-Norwegian margin. On the outer shelf and slope
449 down to the deeper Møre and Vøring basins, the Kai Formation is overall rich in clay and
450 siliceous and calcareous microfossil-bearing pelagic ooze. The sediments of the Kai
451 Formation have largely been redistributed by contour currents (Bryn *et al.* 2005; Laberg *et al.*
452 2005a; Bjordal-Olsen *et al.* 2023). These were related to the opening of the Fram Strait
453 Gateway sometime between 20 and 15 Ma (Jakobsson *et al.* 2007; Engen *et al.* 2008) when
454 extensive deep-water circulation was established between the North Atlantic and Arctic.
455 However, in the Vøring Basin, evidence exist for older contourites, interpreted to originate
456 from ocean circulation also prior to the mid-Miocene (Laberg *et al.* 2005b). The vertical
457 motion history of the Greenland-Iceland-Faroe Ridge (Parnell-Turner *et al.* 2015; Straume *et*
458 *al.* 2020) also had large impact on the ocean circulation in the Norwegian-Greenland Sea and
459 associated depositional processes.

460

461 The new ocean circulation also affected the SW Barents Sea margin where the Bjørnøyrenna
462 Drift (Fig. 2) started to form in the early/middle Miocene (Rydningen *et al.* 2020). The drift
463 is located on the slope and consists of primarily shale with some interfingering sandstones.
464 The sand, however, was probably deposited through turbiditic currents reflecting a complex
465 interplay between down-slope and along-slope sedimentary processes (Rydningen *et al.*
466 2020). The development of this drift was concurrent with Mid-Miocene Climate Optimum (c.
467 16-14 Ma) suggesting a link between ocean circulation and global cooling (Rydningen *et al.*
468 2020).

469

470 During deposition the seafloor bathymetry was affected by large domes and depressions
471 formed during the mid-Miocene compressional tectonic phase, and redistribution of fine-
472 grained sediments commonly took place along the flanks of the domes (Eidvin *et al.* 2014).

473

474 The late Miocene-early Pliocene Molo Formation, characterized by steep clinofolds (Eidvin
475 *et al.* 1998, 2007), was deposited in a coastal shallow marine to prograding deltaic
476 environment, probably formed in a wave-dominated environment with extensive long-shore
477 drift. It is situated on the middle/inner part of the shelf extending about 100 km from the
478 coast off Møre (63°15'N) and north to Lofoten (67°50'N). Based on the recent dates
479 (Grøsfjeld *et al.* 2019; Dybkjær *et al.* 2021) and regional seismic mapping (Bjordal-Olsen *et al.*
480 *et al.* 2023) the Molo Formation is now interpreted to be the proximal equivalent to the deeper
481 marine Kai Formation, deposited as a result of the compression and uplift of mainland
482 Norway in mid-Miocene time (Eidvin *et al.* 2022).

483

484 The main source area for the current-influenced sediments was probably located in the
485 northeast (Lofoten/Vestfjorden area). Significant Neogene uplift and erosion, starting in the
486 Miocene, is reported here (Hendriks and Andriessen 2002; Bjørnseth *et al.* 2003; Redfield *et al.*
487 *et al.* 2005).

488

489 A significant shift in sedimentary processes and depositional environments took place at the
490 Pliocene-Pleistocene transition. Major shelf edge progradation can be linked to grounding of
491 ice sheets on the continental shelf (Andreassen *et al.* 2004, 2008; Dahlgren *et al.* 2005;
492 Andreassen and Winsborrow 2009; Ottesen *et al.* 2009, 2012; Newton and Huuse 2017). The
493 deposition and major progradation of glacial sediments in the North Sea TMF and the trough
494 mouth fans along the western Barents Sea margin were closely linked to the processes
495 shaping the shelves of the North Sea and Barents Sea respectively. Large volumes of glacial
496 sediments were deposited in the Norwegian Sea (and the Nansen Basin in the Arctic) as large
497 fans in front of the bathymetric troughs on the shelf formed by glacial erosion (e.g. Faleide *et al.*
498 *et al.* 1996; Lasabuda *et al.* 2018a; Hjelstuen and Sejrup 2021; Lien *et al.* 2022).

499

500 Over large parts of the Barents Sea shelf there is a distinct composite upper regional
501 unconformity (URU; e.g. Faleide *et al.* 1996). In some areas we observe several
502 unconformities formed in response to individual ice sheets that was grounded and eroded on
503 the shelf. This is more clear on the inner part of the mid-Norwegian (Vøring) margin where

504 upper parts of the Naust Formation reveal several sub-horizontal unconformities (Ottesen *et*
505 *al.* 2009). On the slope, a downlap surface for huge prograding wedges sourced on the
506 mainland and the shelf marks the transition to glacial sediment deposition during the
507 Northern Hemisphere Glaciation since about 2.7 Ma. In terms of total post-breakup sediment
508 volume the glacial component constitutes as much as about 50% on the mid-Norwegian and
509 western Barents Sea margins (Lasabuda *et al.* 2021). The abrupt change in sedimentation rate
510 at the beginning of the Quaternary, increasing by an order of magnitude, cannot be explained
511 by tectonic uplift of landmasses as the main cause. More likely, it reflects climatic change
512 causing effective and significant glacial erosion (Hjelstuen and Sejrup 2021; Patton *et al.*
513 2022).

514
515 The Scandinavian Ice Sheet repeatedly advanced to the shelf edge throughout the Pleistocene
516 (Dahlgren *et al.* 2002; Sejrup *et al.* 2005), and loaded the slopes with thick packages of
517 glacial sediment. Glaciations were initiated a bit earlier (~4 Ma) in the northern Barents
518 Sea/Svalbard area but the first large-scale glaciation reaching the shelf edge did not occur
519 before ~2.75 Ma (Knies *et al.* 2014).

520
521 Continental slope mass failures affected both the North Sea TMF (Nygård *et al.* 2005;
522 Hjelstuen and Andreassen 2015) and Bjørnøya TMF (Hjelstuen *et al.* 2007) and large
523 volumes of slide deposits were transported into the oceanic Norway Basin and Lofoten Basin,
524 respectively (Fig.7). The rapid deposition of glaciogenic sediments at the outer shelf and upper
525 slope contributed to conditions favorable for failure (Hjelstuen *et al.* 2005).

526
527 On the Vøring margin, the latest Pliocene-Pleistocene Naust Formation comprises large
528 quantities of glacially derived material that were transported westwards from the Norwegian
529 mainland and inner shelf and deposited in a basin of intermediate depth as prograding
530 sediment wedges (Dahlgren *et al.* 2002; Rise *et al.* 2005; Ottesen *et al.* 2009, 2012; Newton
531 and Huuse 2017). In this basin, the Helland–Hansen Arch (Fig. 2) acted as a prominent
532 north–south-trending topographic element and affected the deposition of glaciogenic,
533 hemipelagic and contouritic deposits in the early Naust period (Fig. 5; Rise *et al.* 2010;
534 Millett *et al.* 2022).

535
536

537 **Magmatism**

538

539 Voluminous Paleogene volcanism affected the mid-Norwegian margin prior to and during
540 NE Atlantic breakup and initial seafloor spreading between Greenland and Europe and thick
541 piles of extrusive volcanic rocks were emplaced (Planke *et al.* 2000, 2017; Berndt *et al.* 2001;
542 Abdelmalak *et al.* 2016). However, these are not considered part of the prograded margin
543 TSE but form its substrate at the outer margin.

544

545

546 **Heat flow**

547

548 The Møre and Vøring margins have heat flow measurements (both at seabed and in deep
549 exploration wells; Fig. 3A) around 60-65 mW/m², which are typical for “normal” continental
550 areas with no recent tectonic activity. Some lateral variation likely reflects structural
551 complexity (Ritter *et al.* 2004; Pascal 2015).

552

553 The heat flow values at the western Barents Sea margin are generally low except for the
554 abnormally high values (exceeding 1000 mW/m²) associated with the Håkon Mosby mud
555 volcano (Hjelstuen *et al.* 1999; Eldholm *et al.* 1999).

556

557

558 **Petroleum geology**

559

560 The petroleum geology of the pre-breakup CTSE's on the mid-Norwegian margin is well
561 covered by Bunkholt *et al.* (2021) and Faleide *et al.* (2024a), while Ryseth *et al.* (2021) and
562 Faleide *et al.* (2024b) do the same for the western Barents Sea margin. An important source
563 of information is the FactPages of the Norwegian Offshore Directorate
564 (<https://factpages.sodir.no/en>) which is continuously updated with respect to wellbores,
565 discoveries, fields etc. They also present play models for different parts of the Norwegian
566 Continental Shelf (<https://www.sodir.no/en/facts/geology/plays/>).

567

568 *Discovered HC potential*

569

570 No discoveries are yet made within the prograded margins TSE.

571

572 *Current exploration status*

573

574 Exploration activities in the area covered by the Norwegian Sea prograded margins TSE have
575 so far not targeted plays within the prograding sedimentary sequences.

576

577 *Hydrocarbon systems and plays*

578

579 The hydrocarbon systems and plays described for the underlying CTSE's (Bunkholt *et al.*
580 2021; Ryseth *et al.* 2021; Faleide *et al.* 2024a,b) are not applicable to the prograded margins.

581

582 The Norwegian Offshore Directorate has only two potential plays covering the prograded
583 margins (<https://www.sodir.no/en/facts/geology/plays/>). One is unconfirmed and located at
584 the Møre-Vøring marginal highs where fractured volcanic and volcanoclastic rocks could
585 work as reservoir rock. The other builds on the Peon gas field (well 35/2-1; Fig. 3A) found
586 above a prominent angular unconformity within the Norwegian Channel in the northeastern
587 North Sea (Fig. 1B; Bellwald *et al.* 2022). Here, Quaternary glaciofluvial sands forms the
588 reservoir which is sealed by fine-grained glaciomarine sediments and till units (Ottesen *et al.*
589 2012). Similar rocks in a similar setting may exist in the Naust Formation on the mid-
590 Norwegian (Vøring) margin but such a play is not confirmed here.

591

592 In addition, based on studies of recent 3D seismic data covering the outer Vøring and Møre
593 margins (Fig. 3B), Millett *et al.* (2022) presented a range of less conventional plays in
594 Neogene to Quaternary sequences including sand injectites, glacial sands and plays
595 associated with shallow gas hydrates. These are poorly constrained with respect to age,
596 making them difficult to place in the summary chart (Fig. 4).

597

598 *Source rocks.* Mesozoic (Jurassic and Cretaceous) source rocks are present below the mid-
599 Norwegian prograded margin but these are deeply buried and was likely exhausted of any
600 hydrocarbon generation potential at the time of Cenozoic margin progradation. A younger
601 source rock may exist at the outer margin associated with the early Eocene Azolla event
602 (Brinkhuis *et al.* 2006). This may be the source for hydrocarbons generated within the
603 Bjørnøya TMF and methane-venting seep at the seabed of the Håkon Mosby Mud Volcano
604 (Fig. 2) (Hjelstuen *et al.* 1999, Damm and Budéus 2003; Niemann *et al.* 2006; Pape *et al.*
605 2011). Widespread methane seepages are reported along the margin farther north from

606 Bjørnøya to Kongsfjorden on Svalbard (Fig. 1B; [Mau et al. 2017](#); [Weniger et al. 2019](#))
607 indicating working petroleum system(s).

608

609 *Reservoirs.* Sand injectites are widespread within the Kai/Brygge formations on the mid-
610 Norwegian (Vøring) margin ([Millett et al. 2022](#)). Their geometry varies from isolated
611 mounds and saucer-shaped sills to more laterally extensive sills, and these may have reservoir
612 properties. Contourites are interpreted to be present in deeper parts of the North Sea TMF.
613 Some of these may contain sand that could provide reservoir rocks. Quaternary glacial sands
614 may represent shallower exploration targets within the prograded margin ([Millett et al. 2022](#)).

615

616 *Seals.* Fine-grained glacial sediments may have considerable sealing potential related to
617 the plays described above. The thick wedges of glacial debris flows contain large volumes
618 of such sediments that could trap potential reservoir sands mentioned above.

619

620 *Traps.* The Cenozoic compressive anticlines that are widespread on the mid-Norwegian
621 (Vøring) margin form both structural traps with four-way dip closure and combined
622 structural-stratigraphic traps related to their effect on depositional patterns ([Doré and Lundin](#)
623 [1996](#)). However, drilling on some of the domes has so far not been successful. The plays
624 mentioned above related to sand injectites and contourites are eventually associated with
625 stratigraphic traps.

626

627

628

629 **Acknowledgements**

630 We acknowledge the support from the Research Council of Norway through the PALMAR
631 project 336293. MMA also acknowledges support from the 4D NE Atlantic project funded by
632 Vår Energi. Finally, we thank volume editors and the reviewers Haflidi Haflidason and
633 Fridtjof Riis.

634

635 **References**

- 636 Abdelmalak, M.M., Planke, S., Faleide, J., *et al.* 2016. The development of volcanic sequences at rifted
637 margins: New insights from the structure and morphology of the Vøring Escarpment, mid-Norwegian Margin.
638 *Journal of Geophysical Research: Solid Earth*, **121**, 5212–5236. <https://doi.org/10.1002/2015JB012788>
639
- 640 Abdelmalak, M.M., Gac, S., Faleide, J.I., *et al.* 2023. Quantification and restoration of the pre-drift extension
641 across the NE Atlantic conjugate margins during the mid-Permian-early Cenozoic multi-rifting phases.
642 *Tectonics*, **42**, e2022TC007386, <https://doi.org/10.1029/2022TC007386>
643
- 644 Alexandropoulou, N., Winsborrow, M., Andreassen, K., *et al.* 2021. A Continuous Seismostratigraphic
645 Framework for the Western Svalbard-Barents Sea Margin Over the Last 2.7 Ma: Implications for the Late
646 Cenozoic Glacial History of the Svalbard-Barents Sea Ice Sheet. *Front. Earth Sci.* 9:656732.
647 doi: 10.3389/feart.2021.656732
648
- 649 Andreassen, K. and Winsborrow, M. 2009. Signature of ice streaming in Bjørnøyrenna, Polar North Atlantic,
650 through the Pleistocene and implications for ice-stream dynamics. *Annals of Glaciology*, **50**,
651
- 652 Andreassen, K., Nilssen, L.C., Rafaelsen, B. and Kuilman, L. 2004. Three-dimensional seismic data from the
653 Barents Sea margin reveal evidence of past ice streams and their dynamics. *Geology*, **32**, 729-732.
654 doi: 10.1130/G20497.1
655
- 656 Andreassen, K., Laberg, J.S. and Vorren, T.O. 2008. Seafloor geomorphology of the SW Barents Sea and its
657 glaci-dynamic implications. *Geomorphology*, **97**, 157–177. <https://doi.org/10.1016/j.geomorph.2007.02.050>
658
- 659 Baig, I., Faleide, J.I., Jahren, J. and Mondol, N.H. 2016. Cenozoic exhumation on the southwestern Barents
660 Shelf: Estimates and uncertainties constrained from compaction and thermal maturity analyses. *Marine and*
661 *Petroleum Geology*, **73**, 105-130.
662
- 663 Batchelor, C.L., Ottesen, D. and Dowdeswell, J.A. 2017. Quaternary evolution of the northern North Sea margin
664 through glacial debris-flow and contourite deposition. *Journal of Quaternary Science*, **32**, 416–426. DOI:
665 10.1002/jqs.2934
666
- 667 Bellwald, B., Planke, S., Vadakkepuliambatta, S., *et al.* 2022. Quaternary and Neogene Reservoirs of the
668 Norwegian Continental Shelf and the Faroe-Shetland Basin. *First Break*, **40**, 33-44.
669
- 670 Bellwald, B., Manton, B., Lebedeva-Ivanova, N., *et al.* 2024. Rapid glacial sedimentation and overpressure in
671 oozes causing large craters on the mid-Norwegian margin: integrated interpretation of the Naust, Kai and
672 Brygge formations. Geological Society, London, Special Publications, **525**, SP525-2023.
673
- 674 Berg, K., Solheim, A., Bryn, P. 2005. The Pleistocene to recent geological development of the Ormen Lange
675 area. *Marine and Petroleum Geology*, **22**, 45–56. doi:10.1016/j.marpetgeo.2004.10.009
676
- 677 Berndt, C., Planke, S., Alvestad, E., *et al.* 2001. Seismic volcanostratigraphy of the Norwegian Margin:
678 constraints on tectonomagmatic break-up processes. *Journal of the Geological Society of London*, **158**, 413–426,
679 <https://doi.org/10.1144/jgs.158.3.413>
680
- 681 Bjordal-Olsen, S., Rydningen, T.A., Laberg, J.S., *et al.* 2023. Contrasting Neogene–Quaternary continental
682 margin evolution offshore mid-north Norway: Implications for source-to-sink systems. *Marine Geology*, **456**,
683 106974. <https://doi.org/10.1016/j.margeo.2022.106974>
684
- 685 Bjørnseth, H.M., Grant, S.M., Hansen, E.K., *et al.* 1997. Structural evolution of the Vøring Basin, Norway,
686 during the Late Cretaceous and Paleogene. *Journal of the Geological Society of London*, **154**, 559–563.
687 <https://doi.org/10.1144/gsjgs.154.3.0559>
688
- 689 Breivik, A.J., Mjelde, R., Faleide, J.I. and Murai, Y. 2006. Rates of continental breakup magmatism and
690 seafloor spreading in the Norway Basin-Iceland plume interaction. *Journal of Geophysical Research*, **111**
691 (B07102)
692

693 Breivik, A.J., Mjelde, R., Faleide, J.I. and Murai, Y. 2012. The eastern Jan Mayen microcontinent volcanic
694 margin. *Geophysical Journal International*, **188**, 798-818.
695

696 Brekke, H. 2000. The tectonic evolution of the Norwegian Sea Continental Margin with emphasis on the Vøring
697 and Møre Basins. *Geological Society, London, Special Publications*, **167**, 327–378,
698 <https://doi.org/10.1144/GSL.SP.2000.167.01.13>
699

700 Brinkhuis, H., Schouten, S., Collinson, M. E., et al. 2006. Episodic fresh surface waters in the Eocene Arctic
701 Ocean. *Nature*, **441**, 7093, 606-609.
702

703 Bryn, P., Berg, K., Forsberg, C.F., et al. 2005. Explaining the Storegga Slide. *Marine and Petroleum Geology*,
704 **22**, 11–19. <https://doi.org/10.1016/j.marpetgeo.2004.12.003>
705

706 Bunkholt, H.S.S., Oftedal, B.T., Hansen, J.A., et al. 2021. Trøndelag Platform and Halten-Dønna terraces
707 Composite Tectono-Sedimentary Element, Norwegian Sea Rifted Continental Margin. *Geological Society,
708 London, Memoirs*, **57**, <https://10.1144/M57-???>
709

710 Butt, F.A., Drange, H., Elverhøi, A., et al. 2000a. Modelling Late Cenozoic isostatic elevation changes in the
711 Barents Sea and their implications for oceanic and climatic regimes: preliminary results. *Quaternary Science
712 Reviews*, **21**, 1643–1660.
713

714 Butt, F.A., Elverhøi, A., Solheim, A. and Forsberg, C.F. 2000b. Deciphering late Cenozoic evolution of the
715 western Svalbard Margin based of ODP Site 986 results. *Marine Geology*, **169**, 373–390.
716

717 Cohen, K.M., Finney, S.C., Gibbard, P.L. and Fan, J.-X. (2013; updated). The ICS International
718 Chronostratigraphic Chart. *Episodes*, **36**, 199-204.
719

720 Chand, S., Rise, L., Knies, J., et al. 2011. Stratigraphic development of the south Vøring margin (Mid-Norway)
721 since early Cenozoic time and its influence on subsurface fluid flow. *Marine and Petroleum Geology*, **28**, 1350-
722 1363. doi:10.1016/j.marpetgeo.2011.01.005
723

724 Damm, E. and Budéus, G. 2003. Fate of vent-derived methane in seawater above the Håkon Mosby mud
725 volcano (Norwegian Sea). *Marine chemistry*, **82**, 1-11 . doi: 10.1016/S0304-4203(03)00031-8
726

727 Dalland, A., Worsley, D. and Ofstad, K. 1988. A Lithostratigraphical Scheme for the Mesozoic and Cenozoic
728 Succession Offshore Mid- and Northern Norway. *Norwegian Petroleum Directorate Bulletin*, **4**.
729

730 Dahlgren, K.I.T., Vorren, T.O. and Laberg, J.S. 2002. The role of grounding-line sediment supply in ice-sheet
731 advances and growth on continental shelves: An example from the mid-Norwegian sector of the Fennoscandian
732 ice sheet during the Saalian and Weichselian. *Quaternary International*, **95-96**, 25-33.
733

734 Dahlgren, K.I.T., Vorren, T.O., Stoker, M.S., et al. 2005. Late Cenozoic prograding wedges on the NW
735 European continental margin: their formation and relationship to tectonics and climate. *Marine and Petroleum
736 Geology*, **22**, 1089–1110. doi:10.1016/j.marpetgeo.2004.12.008
737

738 Dimakis, P., Braathen, B.I., Faleide, J.I., et al. 1998. Cenozoic erosion and the preglacial uplift of the Svalbard–
739 Barents Sea region. *Tectonophysics*, **300**, 311-327.
740

741 Doré, A.G. and Lundin, E.R. 1996. Cenozoic compressional structures on the NE Atlantic margin: nature,
742 origin and potential significance for hydrocarbon exploration. *Petroleum Geoscience*, **2**, 299-311.
743

744 Doré, A.G., Lundin, E., Jensen, L.N., et al. 1999. Principal tectonic events in the evolution of the northwest
745 European Atlantic margin. *Petroleum Geology Conference Proceedings*, **5**, 41-61.
746

747 Doré, A.G., Lundin, E.R., Kuszniir, N.J. and Pascal, C. 2008. Potential mechanisms for the genesis of Cenozoic
748 domal structures on the NE Atlantic margin: pros, cons and some new ideas. *Geological Society Special
749 Publications*, **306**, 1–26. DOI: 10.1144/SP306.1
750

751 Dybkjær, K., Rasmussen, E.S., Eidvin, T., et al. 2020. A new stratigraphic framework for the Miocene – Lower
752 Pliocene deposits offshore Scandinavia: A multiscale approach. *Geological Journal*, **56**, 1699–1725.

753 DOI: 10.1002/gj.3982
754
755 Eidvin, T., Jansen, E. and Riis, F. 1993. Chronology of Tertiary fan deposits off the western Barents
756 Sea: Implications for the uplift and erosion history of the Barents Shelf. *Marine Geology*, **112**, 109-131.
757
758 Eidvin, T., Goll, R.M., Grogan, P., *et al.* 1998. The Pleistocene to Middle Eocene stratigraphy and geological
759 evolution of the western Barents Sea continental margin at well site 7316/5 –1 (Bjørnøya West area). *Norwegian*
760 *Journal of Geology*, **78**, 99–123.
761
762 Eidvin, T., Jansen, E., Rundberg, Y., *et al.* 2000. The upper Cainozoic of the Norwegian continental shelf
763 correlated with the deep-sea record of the Norwegian Sea and North Atlantic. *Marine and Petroleum Geology*,
764 **17**, 579–600. [https://doi.org/10.1016/S0264-8172\(00\)00008-8](https://doi.org/10.1016/S0264-8172(00)00008-8).
765
766 Eidvin, T., Bugge, T. and Smelror, M. 2007. The Molo Formation, deposited by coastal progradation on
767 the inner Mid-Norwegian continental shelf, coeval with the Kai Formation to the west and the Utsira
768 Formation in the North Sea. *Norwegian Journal of Geology*, **87**, 75–142.
769
770 Eidvin, T., Riis, F. and Rasmussen, E.S. 2014. Correlation of Upper Oligocene to Lower Pliocene deposits of
771 the Norwegian continental shelf, Norwegian Sea, Svalbard, Denmark and their relation to the uplift of
772 Fennoscandia: a synthesis. *Marine and Petroleum Geology*, **56**, 184–221.
773 <https://doi.org/10.1016/j.marpetgeo.2014.04.006>.
774
775 Eidvin, T., Ottesen, D., Dybkjær, K., Rasmussen, E.S. & Riis, F. 2020: The use of Sr isotope stratigraphy to
776 date the Pleistocene sediments of the Norwegian continental shelf – a review. *Norwegian Journal of Geology*
777 **100**, 202013. <https://dx.doi.org/10.17850/njg100-3-1>.
778
779 Eidvin T., Riis, F., Brekke, H. and Smelror, M. 2022. A revised lithostratigraphic scheme for the Eocene to
780 Pleistocene succession on the Norwegian continental shelf. *Norwegian Journal of Geology, Special Publication*,
781 **1**, 1–132, <https://dx.doi.org/10.17850/njgsp1>
782
783 Eiken, O. and Hinz, K. 1993. Contourites in the Fram Strait. *Sedimentary Geology*, **82**, 15–32.
784 [https://doi.org/10.1016/0037-0738\(93\)90110-Q](https://doi.org/10.1016/0037-0738(93)90110-Q)
785
786 Eldholm, O., Thiede, J. and Taylor, B. 1989: Evolution of the Vøring volcanic margin. In: *Proceedings of the*
787 *Ocean Drilling Program, Scientific Results*, **104** 21, College Station, TX (Ocean Drilling Program), 1033–1065.
788 <https://doi.org/10.2973/ODP.PROC.SR.104.191.1989>
789
790 Eldholm, O., Myhre, A.M. and Thiede, J. 1994. Cenozoic tectono-magmatic events in the North Atlantic:
791 potential paleoenvironmental implications. In: Boulter, M.C. & Fischer, H.C. (eds) *Cenozoic Plants and*
792 *Climates of the Arctic*, NA TO ASI Series, 127. Springer-Verlag, Heidelberg, 35-55.
793
794 Eldholm, O., Sundvor, E., Vogt, P.R., *et al.* 1999. SW Barents Sea continental margin heat flow and Hakon
795 Mosby Mud Volcano. *Geo-Marine Letters*, **19**, 29-37.
796
797 Eldholm, O., Tsikalas, F. and Faleide, J.I. 2002. The continental margin off Norway 62-75oN: Palaeogene
798 tectono-magmatic segmentation and sedimentation. *Geological Society Special Publications*, **197**, 39-68.
799
800 Engen, Ø., Faleide, J.I. and Dyreng, T.K. 2008. Opening of the Fram Strait gateway: A review of plate tectonic
801 constraints. *Tectonophysics*, **450**, 51-69.
802
803 Evans, D., Harrison, Z., Shannon, P.M., *et al.* 2005. Palaeoslides and other mass failures of Pliocene to
804 Pleistocene age along the Atlantic continental margin of NW Europe. *Marine and Petroleum Geology*, **22**,
805 1131–1148. doi:10.1016/j.marpetgeo.2005.01.010
806
807 Faleide, J.I., Vågnes, E. and Gudlaugsson, S.T. 1993. Late Mesozoic-Cenozoic evolution of the southwestern
808 Barents Sea in a regional rift-shear tectonic setting. *Marine and Petroleum Geology*, **10**, 186-214.
809
810 Faleide, J.I., Solheim, A., Fiedler, A., Hjelstuen, B.O., *et al.* 1996. Late Cenozoic evolution of the western
811 Barents Sea-Svalbard continental margin. *Global and Planetary Change*, **12**, 53-74.
812

813 Faleide, J.I., Kyrkjebø, R., Kjennerud, T., Gabrielsen, R.H., et al. 2002. Tectonic impact on sedimentary
814 processes during Cenozoic evolution of the northern North Sea and surrounding areas. *Geological Society*
815 *Special Publications*, **196**, 235-269.

816
817 Faleide, J.I., Tsikalas, F., Breivik, A.J., et al. 2008. Structure and evolution of the continental margin off
818 Norway and the Barents Sea. *Episodes*, **31**, 82–91. <http://dx.doi.org/10.18814/epiiugs/2008/v31i1/012>
819

820 Faleide, J.I., Zastrozhnov, D., Abdelmalak, M.M., et al. 2024a. Møre–Vøring Composite Tectono-Sedimentary
821 Element, Norwegian rifted margin, Norwegian Sea. *Geological Society, London, Memoirs*, **57**,
822

823 Faleide, J.I., Wong, P.W., Hassaan, M., et al. 2024b. West Barents Shear Margin Composite Tectono-
824 Sedimentary Element. *Geological Society, London, Memoirs*, **57**,
825

826 Fiedler, A. and Faleide, J.I. 1996. Cenozoic sedimentation along the southwestern Barents Sea
827 margin in relation to uplift and erosion of the shelf. *Global and Planetary Change*, **12**, 75-93.
828

829 Forsberg, C.F., Solheim, A., Elverhøi, A., et al. 1999. The depositional environment of the western Svalbard
830 margin during the late Pliocene and the Pleistocene: Sedimentary facies changes at Site 986. *Proceedings of the*
831 *Ocean Drilling Program: Scientific Results*, **162**, 233-246.
832

833 Funck, T., Geissler, W.H., Kimbell, G.S., et al. 2017, Moho and basement depth in the NE Atlantic Ocean based
834 on seismic refraction data and receiver functions. Geological Society, London, Special Publications, **447**, 207-
835 231.
836

837 Gabrielsen, R.H., Giannenas, P.A., Sokoutis, D., et al. 2023. Analogue experiments on releasing and restraining
838 bends and their application to the study of the Barents Shear Margin. *Solid Earth*, **14**, 961–983.
839

840 Gac, S., Klitzke, P., Minakov, A., Faleide, J.I. and Scheck-Wenderoth, M. (2016) Lithospheric strength and
841 elastic thickness of the Barents Sea and Kara Sea region. *Tectonophysics*, **691**, 120-132.
842

843 Gaina, C., Gernigon, L. and Ball, P. 2009. Palaeocene–Recent plate boundaries in the NE Atlantic and the
844 formation of the Jan Mayen microcontinent. *Journal of the Geological Society, London*, **166**, 601–616.
845 doi: 10.1144/0016-76492008-112.
846

847 Gernigon, L., Zastrozhnov, D., Planke, S., et al. 2021. A digital compilation of structural and magmatic
848 elements of the Mid-Norwegian continental margin (version 1.0). *Norwegian Journal of Geology*, **101**.
849

850 Green, P.F. and Duddy, I.R. 2010. Synchronous exhumation events around the Arctic including examples
851 from Barents Sea and Alaska North Slope. *Petroleum Geology Conference Proceedings*, **7**, 633-644.
852

853 Grogan, P., Østvedt-Ghazi, A.-M., Larsen, G.B., et al. 1999. Structural elements and petroleum geology of the
854 Norwegian sector of the northern Barents Sea. *Geological Society Petroleum Geology Conference Series*, **5**,
855 247-259.
856

857 Grøsfjeld, K., Dybkjær, K., and Eidvin, T., et al. 2019. A Miocene age for the Molo Formation, Norwegian Sea
858 shelf off Vestfjorden, based on marine palynology. *Norwegian Journal of Geology*, **99**,
859

860 Haflidason, H., Sejrup, H.P., Nygård, A., et al. 2004. The Storegga Slide: architecture, geometry and slide
861 development. *Marine Geology*, **213**, 201–234. doi:10.1016/j.margeo.2004.10.007
862

863 Haflidason, H., Lien, R., Sejrup, H.P., et al. 2005. The dating and morphometry of the Storegga Slide. *Marine*
864 *and Petroleum Geology*, **22**, 123-136. <https://doi.org/10.1016/j.marpetgeo.2004.10.008>
865

866 Hendriks, B., Andriessen, P., Huigen, Y., et al. 2007. A fission track data compilation for Fennoscandia
867 *Norwegian Journal of Geology*, **87**, 143-155.
868

869 Henriksen, S., Fichler, C., Grønlie, A., et al. 2005. The Norwegian Sea during the Cenozoic. *NPF Special*
870 *Publication*, **12**, 111-133.
871

872 Henriksen, E., Bjørnseth, H.M., Hals, T.K., *et al.* 2011. Chapter 17: Uplift and erosion of the greater Barents
873 Sea: impact on prospectivity and petroleum systems. Geological Society, London, Memoirs, 35, 271-281.
874

875 Hjelstuen, B.O. and Andreassen, E.V. 2015. North Atlantic Ocean deep-water processes and depositional
876 environments: A study of the Cenozoic Norway Basin. *Marine and Petroleum Geology*, **59**, 429-441.
877 <http://dx.doi.org/10.1016/j.marpetgeo.2014.09.011>
878

879 Hjelstuen, B.O. and Grinde, S. 2016. 3D Seismic Investigations of Pleistocene Mass Transport Deposits and
880 Glacigenic Debris Flows on the North Sea Fan, NE Atlantic Margin. In: G. Lamarche et al. (eds.), Submarine
881 Mass Movements and their Consequences, *Advances in Natural and Technological Hazards Research*, **41**,
882 DOI 10.1007/978-3-319-20979-1_26
883

884 Hjelstuen, B.O. and Sejrup, H.P. 2021. Latitudinal variability in the Quaternary development of the Eurasian ice
885 sheets - Evidence from the marine domain. *Geology*, **49**, 346-351.
886

887 Hjelstuen, B.O., Elverhøi, A. and Faleide, J.I. 1996. Cenozoic erosion and sediment yield in the drainage area of
888 the Storfjorden Fan. *Global and Planetary Change*, **12**, 95-117.
889

890 Hjelstuen, B.O., Eldholm O. and Skogseid, J. 1997. Vøring Plateau diapir fields and their structural and
891 depositional settings. *Marine Geology*, **144**, 33-57.
892

893 Hjelstuen, B.O., Eldholm, O. and Skogseid, J. 1999. Cenozoic evolution of the northern Vøring margin.
894 *Geological Society of America Bulletin*, **111**, 1792-1807,
895 [https://doi.org/10.1130/0016-7606\(1999\)111%3C1792:CEOTNV%3E2.3.CO;2](https://doi.org/10.1130/0016-7606(1999)111%3C1792:CEOTNV%3E2.3.CO;2)
896

897 Hjelstuen, B., Eldholm, O., Faleide, J.I. and Vogt, P. 1999. Regional setting of the Håkon Mosby Mud Volcano,
898 SW Barents Sea Margin. *Geo-Marine Letters*, **19**, 22-28.
899

900 Hjelstuen, B.O., Sejrup, H.P., Haflidason, H., *et al.* 2005. Late Cenozoic glacial history and evolution of the
901 Storegga Slide area and adjacent slide flank regions, Norwegian continental margin. *Marine and Petroleum*
902 *Geology*, **22**, 57-69. doi:10.1016/j.marpetgeo.2004.10.002
903

904 Hjelstuen, B.O., Eldholm, O. and Faleide, J.I. 2007. Recurrent Pleistocene mega-failures on the SW Barents Sea
905 margin. *Earth and Planetary Science Letters*, **258**, 605-618.
906

907 Jakobsson, M., Backman, J., Rudels, B., *et al.* 2007. The early Miocene onset of a ventilated circulation regime
908 in the Arctic Ocean. *Nature*, **447**, 986-990.
909

910 Jakobsson, M., Mayer, L. A., *et al.* 2020. The International Bathymetric Chart of the Arctic Ocean Version 4.0.
911 *Scientific Data*, **7**, 1, 176.
912

913 Jebson, C. and Faleide, J.I. 1998. Tertiary rifting and magmatism at the western Barents Sea margin
914 (Vestbakken Volcanic Province). Third Int. Conf. on Arctic Margins, Celle, Germany, 12-16.10, 1998.
915

916 King, E.L., Sejrup, H.P., Haflidason, H., Elverhøi, A. and Aarseth, I., 1996, Quaternary seismic stratigraphy of
917 the North Sea Fan: glacially-fed gravity flow aprons, hemipelagic sediments and large submarine slides. *Marine*
918 *Geology*, **130**, 295-315. [https://doi.org/10.1016/0025-3227\(95\)00168-9](https://doi.org/10.1016/0025-3227(95)00168-9)
919

920 Knies, J., Matthiessen, J., Vogt, C., *et al.* 2009. The Plio-Pleistocene glaciation of the Barents Sea-Svalbard
921 region: A new model based on revised chronostratigraphy. *Quaternary Science Reviews*, **28**, 812-829.
922 <https://doi.org/10.1016/j.quascirev.2008.12.002>
923

924 Knies, J., Mattingsdal, R., Fabian, K., *et al.* 2014. Effect of early Pliocene uplift on late Pliocene cooling in the
925 Arctic-Atlantic gateway. *Earth and Planetary Science Letters*, **387**, 132-144.
926 <https://doi.org/10.1016/j.epsl.2013.11.007>
927

928 Ktenas, D., Henriksen, E., Meisingset, I., *et al.* 2017. Quantification of the magnitude of net erosion in the
929 Southwest Barents Sea using sonic velocities and compaction trends in shales and sandstones. *Marine and*
930 *Petroleum Geology*, **88**, 826-844.
931

932 Ktenas, D., Meisingset, I., Henriksen, E. and Nielsen, J.K., 2019. Estimation of net apparent erosion in the SW
933 Barents Sea by applying velocity inversion analysis. *Petroleum Geoscience*, **25**, 169–187.
934
935 Ktenas, D., Nielsen, J.K., Henriksen, E., *et al.* 2023. The effects of uplift and erosion on the petroleum systems
936 in the southwestern Barents Sea: Insights from seismic data and 2D petroleum systems modelling. *Marine and*
937 *Petroleum Geology*, **158**, 106535.
938
939 Kuvaas, B. and Kristoffersen, Y. 1996. Mass movements in glaciomarine sediments on the Barents Sea
940 continental slope. *Global and Planetary Change*, **12**, 287-307.
941
942 Kvalstad, T.J., Andresen, L., Forsberg, C.F., *et al.* 2005a. The Storegga slide: evaluation of triggering sources
943 and slide mechanics. *Marine and Petroleum Geology*, **22**, 245–256.
944 doi:10.1016/j.marpetgeo.2004.10.019
945
946 Kvalstad, T.J., Nadim, F., Kaynia, A.M., *et al.* 2005b. Soil conditions and slope stability in the Ormen Lange
947 area. *Marine and Petroleum Geology*, **22**, 299–310. doi:10.1016/j.marpetgeo.2004.10.021
948
949 Laberg, J.S. and Vorren, T.O. 1993. A Late Pleistocene submarine slide on the Bear Island Trough Mouth Fan.
950 *Geo-Marine Letters*, **13**, 227-234.
951
952 Laberg, J.S. and Vorren, T.O. 1996. The middle and late Pleistocene evolution of the Bear Island Trough Mouth
953 Fan. *Global and Planetary Change*, **12**, 309-330.
954
955 Laberg, J.S. and Vorren, T.O. 2000. Flow behaviour of the submarine glacial debris flows on the Bear Island
956 Trough Mouth Fan, western Barents Sea. *Sedimentology*, **47**, 1105-1117.
957
958 Laberg, J.S., Vorren, T.O., Mienert, J., *et al.* 2002. Late Quaternary palaeoenvironment and chronology in the
959 Trænadjupet Slide area offshore Norway. *Marine Geology*, **188**, 35-60.
960
961 Laberg, J.S., Stoker, M.S., Dahlgren, K.I.T., *et al.* 2005a. Cenozoic alongslope processes and sedimentation
962 on the NW European Atlantic margin. *Marine and Petroleum Geology*, **22**, 1069–1088.
963 doi:10.1016/j.marpetgeo.2005.01.008
964
965 Laberg, J.S., Dahlgren, K.I.T. and Vorren, T.O. 2005b. The Eocene–late Pliocene paleoenvironment in the
966 Vøring Plateau area, Norwegian Sea - paleoceanographic implications. *Marine Geology*, **214**, 269-285.
967
968 Laberg, J.S., Andreassen, K., Knies, J., *et al.* 2010. Late Pliocene–Pleistocene development of the Barents Sea
969 ice sheet. *Geology*, **38**, 107–110. <https://doi.org/10.1130/G30193.1>
970
971 Laberg, J.S., Andreassen, K. and Tore O. Vorren, T.O. 2012. Late Cenozoic erosion of the high-latitude
972 southwestern Barents Sea shelf revisited. *GSA Bulletin*, **124**, 77–88; doi: 10.1130/B30340.1
973
974 Lasabuda, A., Laberg, J.S., Knutsen, S.-M. and Safronova, P.A. 2018a. Cenozoic tectonostratigraphy and pre-
975 glacial erosion: a mass-balance study of the northwestern Barents Sea margin, Norwegian Arctic. *Journal of*
976 *Geodynamics*, **119**, 149-166, <https://doi.org/10.1016/j.jog.2018.03.004>
977
978 Lasabuda, A., Laberg, J.S., Knutsen, S.-M. and Høgseth, G. 2018b. Early to middle Cenozoic paleoenvironment
979 and erosion estimates of the southwestern Barents Sea: Insights from a regional mass-balance approach. *Mar.*
980 *Pet. Geol.*, **96**, 501–521, <https://doi.org/10.1016/j.marpetgeo.2018.05.039>.
981
982 Lasabuda, A.P., Johansen, N.S., Laberg, J.S., Faleide, J.I., *et al.* 2021 Cenozoic uplift and erosion of the
983 Norwegian Barents Shelf—a review. *Earth-Science Reviews*, **217**, 103609.
984
985 Lidmar-Bergström, K., Näslund, J.-O., Ebert, K., *et al.* 2007 Cenozoic landscape development in northern
986 Scandinavia. *Norwegian Journal of Geology*, **87**, 181-196.
987
988 Lien, Ø.F., Hjelstuen, B.O., Zhang, X. and Sejrup, H.P. 2022. Late Plio-Pleistocene evolution of the Eurasian
989 Ice Sheets inferred from sediment input along the northeastern Atlantic continental margin. *Quaternary Science*
990 *Reviews*, **282**, 107433. <https://doi.org/10.1016/j.quascirev.2022.107433>
991

992 Ljones, F., Kuwano, A., Mjelde, R., *et al.* 2004. Crustal transect from the North Atlantic Knipovich Ridge to the
993 Svalbard Margin west of Hornsund. *Tectonophysics*, **378**, 17-41.
994
995 Lundin, E.R. and Doré, A.G. 2002. Mid-Cenozoic post-breakup deformation in the ‘passive’ margins bordering
996 the Norwegian- Greenland Sea. *Marine and Petroleum Geology*, **19**, 79–93.
997
998 Lundin, E.R., Doré, A.G., Rønning, K. and Kyrkjebø, R. 2013. Repeated inversion and collapse in the Late
999 Cretaceous–Cenozoic northern Vøring Basin, offshore Norway. *Petroleum Geoscience*, **19**, 329–341.
1000 doi: 10.1144/petgeo2012-022
1001
1002 Løseth, H., Kyrkjebø, R., Hilde, E., *et al.* 2017. 500 m of rapid base level rise along an inner passive margin–
1003 Seismic observations from the Pliocene Molo Formation, mid Norway. *Marine and Petroleum Geology*, **86**,
1004 268–287. <https://doi.org/10.1016/j.marpetgeo.2017.05.039>.
1005
1006 Martinsen, O.J., Bøen, F., Charnock, M.A., *et al.* 1999. Cenozoic development of the Norwegian margin 60-
1007 64°N: sequences and sedimentary response to variable basin physiography and tectonic setting. *Geological*
1008 *Society Petroleum Geology Conference Series*, **5**, 293-304.
1009
1010 Mau, S., Römer, M., Torres, M.E., *et al.* 2017. Widespread methane seepage along the continental margin
1011 off Svalbard - from Bjørnøya to Kongsfjorden. *Nature Scientific Reports*, **7**:42997. DOI: 10.1038/srep42997
1012
1013 Maus, S., Barckhausen, U., Berkenbosch, H., *et al.* 2009. EMAG2: A 2-arc min resolution Earth Magnetic
1014 Anomaly Grid compiled from satellite, airborne, and marine magnetic measurements. *Geochemistry*,
1015 *Geophysics, Geosystems*, **10**, Q08005.
1016
1017 Maystrenko, Y.P., Olesen, O., Gernigon, L. and Gradmann, S. 2017. Deep structure of the Lofoten-Vesterålen
1018 segment of the Mid-Norwegian continental margin and adjacent areas derived from 3-D density modeling:
1019 *Journal of Geophysical Research: Solid Earth*, **122**, 1402-1433.
1020
1021 Medvedev, S., Faleide, J.I. and Hartz, E. 2022. Cenozoic reshaping of the Barents-Kara Shelf: Influence of
1022 erosion, sedimentation, and glaciation. *Geomorphology*, **420**, 108500
1023
1024 Meza-Cala, J.C., Tsikalas, F., Faleide, J.I. and Abdelmalak, M.M. 2021. New insights into the late Mesozoic-
1025 Cenozoic tectono-stratigraphic evolution of the northern Lofoten-Vesterålen margin, offshore Norway. *Marine*
1026 *and Petroleum Geology*, **134**, 105370.
1027
1028 Millett, J.M., Manton, B.M., Zastrozhnov, D., *et al.* 2022. Basin Structure and Prospectivity of the NE Atlantic
1029 Volcanic Rifted Margin: Cross-border examples from the Faroe-Shetland, Møre and Southern Vøring Basins.
1030 *Geological Society of London, Special Publications*, **495**, 99–138, <https://doi.org/10.1144/SP495-2019-12>
1031
1032 Mosar, J., Lewis, G. and Torsvik, T.H. 2002. North Atlantic sea-floor spreading rates: implications for the
1033 Tertiary development of inversion structures of the Norwegian–Greenland Sea. *Journal of the Geological*
1034 *Society, London*, **159**, 503–515.
1035
1036 Nasuti, A. and Olesen, O. 2014. Magnetic data. In: Hopper, J.R., Funck, T., Stoker, M.S., *et al.* (eds)
1037 Tectonostratigraphic Atlas of the North-East Atlantic Region. GEUS, Copenhagen, Denmark, 41-52.
1038
1039 Newton, A.M.W. and Huuse, M. 2017. Late Cenozoic environmental changes along the Norwegian margin.
1040 *Marine Geology*, **393**, 216-244. <http://dx.doi.org/10.1016/j.margeo.2017.05.004>
1041
1042 Niemann, H., Lösekann, T., de Beer, D., *et al.* 2006. Novel microbial communities of the Haakon Mosby
1043 mud volcano and their role as a methane sink. *Nature*, 443, 19 October 2006. Doi:10.1038/nature05227
1044
1045 Nygård, A., Sejrup, H.P., Haflidason, H. and Bryn, P. 2005. The glacial North Sea Fan, southern Norwegian
1046 Margin: architecture and evolution from the upper continental slope to the deep-sea basin. *Marine and*
1047 *Petroleum Geology*, **22**, 71–84. doi:10.1016/j.marpetgeo.2004.12.001
1048
1049 Olesen, O., Brønner, M. *et al.* 2010. New aeromagnetic and gravity compilations from Norway and adjacent
1050 areas: methods and applications. *Geological Society, London, Petroleum Geology Conference Series*, **7**, 559–
1051 586, <https://doi.org/10.1144/0070559>

1052
1053 Ottesen, D., Dowdeswell, J.A., Rise, L., *et al.* 2002. Large-scale morphological evidence for past ice-stream
1054 flow on the mid-Norwegian continental margin. *Geological Society Special Publications*, **203**, 245-258.
1055
1056 Ottesen, D., Dowdeswell, J. A. and Rise, L. 2005. Submarine landforms and the reconstruction of fastflowing
1057 ice streams within a large Quaternary ice sheet: the 2500 km-long Norwegian–Svalbard margin (57 to 80 N).
1058 *Geological Society of America Bulletin*, **117**, 1033–1050.
1059
1060 Ottesen, D., Rise, L., Andersen, E. S., Bugge, T. and Eidvin, T. 2009. Geological evolution of the Norwegian
1061 continental shelf between 61N and 68N during the last 3 million years. *Norwegian Journal of Geology*, **89**, 251–
1062 265.
1063
1064 Ottesen, D., Dowdeswell, J.A., Rise, L. and Bugge, T. 2012. Large-scale development of the mid-Norwegian
1065 shelf over the last three million years and potential for hydrocarbon reservoirs in glacial sediments. *Geological
1066 Society Special Publications*, **368**, doi 10.1144/SP368.6
1067
1068 Pape, T., Feseker, T., Kasten, S., *et al.* 2011. Distribution and abundance of gas hydrates in near-surface
1069 deposits of the Håkon Mosby Mud Volcano, SW Barents Sea. *G-cube*, **12**. doi:10.1029/2011GC003575
1070
1071 Parnell-Turner, R., White, N.J., McCave, I.N., *et al.* 2015. Architecture of North Atlantic contourite drifts
1072 modified by transient circulation of the Icelandic mantle plume. *Geochemistry, Geophysics, Geosystems*, **16**,
1073 3414-3435.
1074
1075 Pascal, C. 2015. Heat flow of Norway and its continental shelf. *Marine and Petroleum Geology*, **66**, 956-969,
1076 <http://dx.doi.org/10.1016/j.marpetgeo.2015.08.006>
1077
1078 Patton, H., Hubbard, A., Heyman, J., *et al.* 2022. The extreme yet transient nature of glacial erosion. *Nature
1079 Communications*, **13**:7377. <https://doi.org/10.1038/s41467-022-35072-0>
1080
1081 Planke, S., Symonds, P.A., Alvestad, E. and Skogseid, J. 2000. Seismic volcanostratigraphy of large-volume
1082 basaltic extrusive complexes on rifted margins. *Journal of Geophysical Research - Solid Earth*, **105**, 19335–
1083 19351. <https://doi.org/10.1029/1999JB900005>
1084
1085 Planke, S., Millett, J.M., Maharjan, D., *et al.* 2017. Igneous seismic geomorphology of buried lava fields and
1086 coastal escarpments on the Vøring volcanic rifted margin. *Interpretation*, **5**, 1–42.
1087
1088 Planke, S., Berndt, C., Alvarez Zarikian, C.A., and the Expedition 396 Scientists 2023. Expedition 396
1089 summary. *Proceedings of the International Ocean Discovery Program*, Volume **396**, publications.iodp.org
1090
1091 Praeg, D., Stoker, M.S., Shannon, P.M., *et al.* 2005. Episodic Cenozoic tectonism and the development of the
1092 NW European ‘passive’ continental margin. *Marine and Petroleum Geology*, **22**, 1007–1030.
1093 doi:10.1016/j.marpetgeo.2005.03.014
1094
1095 Rebesco, M., Hernández-Molina, F.J., Van Rooij, D. and Wåhlin, A. 2014. Contourites and associated
1096 sediments controlled by deep-water circulation processes: State-of-the-art and future considerations. *Marine
1097 Geology*, **352**, 11-154.
1098
1099 Redfield, T. and Osmundsen, P.T. 2013. The long-term topographic response of a continent adjacent to
1100 a hyperextended margin: A case study from Scandinavia. *GSA Bulletin*, **125**, 184–200. doi:10.1130/B30691.1
1101
1102 Richardsen, G., Henriksen, E. and Vorren, T.O. 1991. Evolution of the Cenozoic sedimentary wedge during
1103 rifting and seafloor spreading west of the Stappen High, western Barents Sea. *Marine Geology*, **101**, 11-30.
1104
1105 Riis, F., Berg, K., Cartwright, J., *et al.* 2005. Formation of large, crater-like evacuation structures in ooze
1106 sediments in the Norwegian Sea. Possible implications for the development of the Storegga Slide. *Marine and
1107 Petroleum Geology*, **22**, 257–273. doi:10.1016/j.marpetgeo.2004.10.023
1108
1109 Rise, L. and Sættem, J. 1994. Shallow stratigraphic wireline coring in bedrock offshore Norway. *Scientific
1110 Drilling*, **4**, 243-257.
1111

1112 Rise, L., Ottesen, D., Berg, K. and Lundin, E. 2005. Large-scale development of the mid-Norwegian
1113 margin during the last 3 million years. *Marine and Petroleum Geology*, **22**, 33–44.
1114

1115 Rise, L., Ottesen, D., Longva, O., *et al.* 2006. The Sklinnadjupet slide and its relation to the Elsterian glaciation
1116 on the mid-Norwegian margin. *Marine and Petroleum Geology*, **23**, 569–583.
1117

1118 Rise, L., Chand, S., Hjelstuen, B.O., *et al.* 2010. Late Cenozoic geological development of the south Vøring
1119 margin, mid-Norway. *Marine and Petroleum Geology*, **27**, 1789-1803. doi:10.1016/j.marpetgeo.2010.09.001
1120

1121 Rise, L., Bøe, R., Riis, F., *et al.* 2013. The Lofoten-Vesterålen continental margin, North Norway: Canyons and
1122 mass-movement activity. *Marine and Petroleum Geology*, **45**, 134-149.
1123

1124 Ritter, U., Zielinski, G.R., Weiss, H.M., *et al.* 2004. Heat flow in the Vøring Basin, Mid-Norwegian Shelf.
1125 *Petroleum Geoscience*, **10**, 353–365, <https://doi.org/10.1144/1354-079303-616>
1126

1127 Rydningen, T.A., Høgseth, G.V., Lasabuda, A.P.E., Laberg, J.S., *et al.* 2020. An early Neogene—Early
1128 Quaternary contourite drift system on the SW Barents Sea continental margin, Norwegian Arctic. *G-cube*, **21**,
1129 e2020GC009142. <https://doi.org/10.1029/2020GC009142>
1130

1131 Ryseth, A.E., Augustson, J.H., Charnock, M., *et al.* 2003. Cenozoic stratigraphy and evolution of the
1132 Sørvestsnaget Basin, southwest Barents Sea. *Norwegian Journal of Geology*, **83**, 107–130.
1133

1134 Ryseth, A.E., Similox-Tohon, D. and Thießen, O. 2021. Tromsø–Bjørnøya Composite Tectono-Sedimentary
1135 Element, Barents Sea. Geological Society, London, Memoirs, **57**, <https://doi.org/10.1144/M57-2018-19>
1136

1137 Safronova, P.A., Laberg, J.S., Andreassen, K., *et al.* 2017. Late Pliocene–early Pleistocene deep-sea basin
1138 sedimentation at high-latitudes: mega-scale submarine slides of the north-western Barents Sea margin prior to
1139 the shelf-edge glaciations. *Basin Research*, **29**, 537-555.
1140

1141 Sejrup, H.P., Larsen, E., Haflidason, H., *et al.* 2003. Configuration, history and impact of the Norwegian
1142 Channel Ice Stream. *Boreas*, **32**, 18–36. <https://doi.org/10.1080/03009480310001029>
1143

1144 Sejrup, H.P., Hjelstuen, B.O., Dahlgren, K.I.T., *et al.* 2005. Pleistocene glacial history of the NW European
1145 continental margin. *Marine and Petroleum Geology*, **22**, 1111–1129. doi:10.1016/j.marpetgeo.2004.09.007
1146

1147 Skilbrei, J.R., Kihle, O., Olesen, O., *et al.* 2000. Gravity anomaly map Norway and adjacent ocean areas, scale
1148 1:3 Million, Geological Survey of Norway, Trondheim.
1149

1150 Skogseid, J., Planke, S., Faleide, J.I., *et al.* 2000. NE Atlantic continental rifting and volcanic margin formation.
1151 *Geological Society Special Publications*, **167**, 295–326, <https://doi.org/10.1144/GSL.SP.2000.167.01.12>
1152

1153 Solheim, A., Faleide, J.I., Andersen, E.S., *et al.* 1998. Late Cenozoic seismic stratigraphy and glacial geological
1154 development of the East Greenland and Svalbard–Barents Sea continental margins. *Quat. Sci. Rev.* **17**, 155–184.
1155

1156 Solheim, A., Berg, K., Forsberg, C.F. and Bryn, P. 2005. The Storegga Slide complex: repetitive large scale
1157 sliding with similar cause and development. *Marine and Petroleum Geology*, **22**, 97–107.
1158 doi:10.1016/j.marpetgeo.2004.10.013
1159

1160 Stoker, M.S., Praeg, D., Shannon, P.M., *et al.* 2005a. Neogene evolution of the Atlantic continental margin of
1161 NW Europe (Lofoten Islands to SW Ireland): anything but passive. *Geological Society, London, Petroleum
1162 Geology Conference Series*, **6**, 1057–1076.
1163

1164 Stoker, M.S., Hout, R.J., Nielsen, T., *et al.* 2005b. Sedimentary and oceanographic responses to early Neogene
1165 compression on the NW European margin. *Marine and Petroleum Geology*, **22**.
1166 doi: 10.1016/j.marpetgeo.2005.01.009.
1167

1168 Stoker, M.S., Praeg, D., Hjelstuen, B.O., Laberg, J.S., *et al.* 2005c. Neogene stratigraphy and the sedimentary
1169 and oceanographic development of the NW European Atlantic margin. *Marine and Petroleum Geology*, **22**,
1170 977–1005. doi:10.1016/j.marpetgeo.2004.11.007
1171

1172 Straume, E.O., Gaina, C., Medvedev, S. and Nisancioglu, K.H. 2020. Global Cenozoic Paleobathymetry with a
1173 focus on the Northern Hemisphere Oceanic Gateways. *Gondwana Research*, **86**, 126–143.
1174 <https://doi.org/10.1016/j.gr.2020.05.011>
1175

1176 Stuevold, L.M. and Eldholm, O. 1996. Cenozoic uplift of Fennoscandia inferred from a study of the
1177 mid-Norwegian margin. *Global and Planetary Change*, **12**, 359-386.
1178

1179 Sættem, J., Bugge, T., Fanavoll, S., *et al.* 1994. Cenozoic margin development and erosion of the Barents Sea:
1180 Core evidence from southwest of Bjørnøya. *Marine Geology*, **118**, 257-281.
1181

1182 Talwani, M., Udintsev, G. and White S.M. 1976. Introduction and Explanatory Notes, Leg 38, Deep Sea
1183 Drilling Project. doi:10.2973/dsdp.proc.38.101.1976.
1184

1185 Thiede, J., Eldholm, O. and Taylor, E. 1989. Variability of Cenozoic Norwegian-Greenland Sea
1186 paleoceanography and northern hemisphere paleoclimate. Proceedings of the Ocean Drilling Program, Scientific
1187 Results, 104, 1067-118.
1188

1189 Tsikalas, F., Meza-Cala, J.C., Abdelmalak, M.M., *et al.* 2022. Lofoten Composite Tectono-Sedimentary
1190 Element, Norwegian Rifted Margin, Norwegian Sea. *Geological Society of London, Memoirs*, **57**,
1191

1192 Verhoef, J., Roest, W. R., MacNab, R., *et al.* 1996. Magnetic anomalies of the Arctic and North Atlantic Oceans
1193 and adjacent land areas. Geological Survey Canada Open File 3125a.
1194

1195 Vorren, T.O., Lebesbye, E., Andreassen, K. and Larsen, K.-B. 1989. Glacigenic sediments on a passive
1196 continental margin as exemplified by the Barents Sea. *Marine Geology*, **85**, 251-272.
1197

1198 Vorren, T.O., Richardsen, G., Knutsen, S.M. and Henriksen, E. 1991. Cenozoic erosion and sedimentation in the
1199 western Barents Sea. *Marine and Petroleum Geology*, **8**, 317-340.
1200

1201 Vorren, T.O., Laberg, J.S., Blaume, F., *et al.* 1998, The Norwegian-Greenland Sea continental margins:
1202 Morphology and Late Quaternary Sedimentary processes and environment: Quaternary Science Reviews, v. 17,
1203 p. 273-302, [https://doi.org/10.1016/S0277-3791\(97\)00072-3](https://doi.org/10.1016/S0277-3791(97)00072-3).
1204

1205 Vågnes, E., Gabrielsen, R.H. and Haremo, P. 1998. Late Cretaceous–Cenozoic intraplate contractional
1206 deformation at the Norwegian continental shelf: timing, magnitude and regional implications. *Tectonophysics*,
1207 **300**, 29–46.
1208

1209 Weniger, P., Blumenberg, M., Berglar, K., *et al.* 2019. Origin of near-surface hydrocarbon gases bound in
1210 northern Barents Sea sediments. *Marine and Petroleum Geology*, **102**, 455-476.
1211

1212 Zastrozhnov, D., Gernigon, L., Gogin, I., *et al.* 2020, Regional structure and polyphased Cretaceous-Paleocene
1213 rift and basin development of the mid-Norwegian volcanic passive margin. *Marine and Petroleum Geology*,
1214 **115**, 104269.
1215

1216

1217 **Figure captions**

1218

1219 Figure 1: (A) Regional North Atlantic-Arctic setting and location of study area. (B) Study
1220 area with outline of the Norwegian Sea Oceanic Basin and Prograded Margins Composite
1221 Tectono-Sedimentary Element. Outline of other CTSE's also shown. Topography and
1222 bathymetry from IBCAO (Jakobsson et al. 2020) and oceanic structure based on Abdelmalak
1223 et al. (2023). Bj, Bjørnøya; FS, Fram Strait; EGFZ, East Greenland Fracture Zone; GIFR,
1224 Greenland-Iceland-Faroe Ridge; KB, Kolbeinsey Ridge; Kfj, Kongsfjorden; KR, Knipovich
1225 Ridge; LVM, Lofoten-Vesterålen Margin; NC, Norwegian Channel; ÆR, Ægir Ridge.

1226

1227 Figure 2: Breakup-related volcanics underlying the prograded margins (Gernigon et al. 2021).
1228 Outline of the Norwegian Sea Oceanic Basin and Prograded Margins CTSE. Oceanic
1229 structure based on Abdelmalak et al. (2023). Also shown are Cenozoic domes/arches
1230 (Gernigon et al. 2021), Cenozoic sediment drifts (Bjordal-Olsen 2023) and location of
1231 profiles in Figs. 5 and 8. BeD, Bellsund Drift; Bj, Bjørnøya; BrD, Bjørnøyrenna Drift; FS,
1232 EGFZ, East Greenland Fracture Zone; HHA, Helland-Hansen Arch; HMMV, Håkon Mosby
1233 Mud Volcano; ID, Isfjorden Drift; JMC, Jan Mayen Corridor; JMFZ, Jan Mayen Fracture
1234 Zone; Kfj, Kongsfjorden; KR, Knipovich Ridge; LD, Lofoten Drift; LVM, Lofoten-
1235 Vesterålen Margin; MA, Modgun Arch; ND, Naglfar Dome; NC, Norwegian Channel; NyD,
1236 Nyk Drift; OLD, Ormen Lange Dome; SD, Sklinnadjupet Drift; VD, Vema Dome; VeD,
1237 Vesterålen Drift; VVP, Vestbakken Volcanic Province; WSD, West Shetland Drift; ÆR,
1238 Ægir Ridge.

1239

1240 Figure 3: Data coverage. (A) Location of exploration wells and scientific/shallow
1241 stratigraphic boreholes. Key wells are highlighted and labelled. Location of heat flow
1242 measurements also shown; (B) Seismic data – regional 2D seismic reflection profiles in thin
1243 grey lines, 3D seismic cubes in colour polygons, thick red lines show deep seismic refraction
1244 data. CTSE outline shown in both maps. Oceanic structure based on Abdelmalak et al.
1245 (2023). EGFZ, East Greenland Fracture Zone; JMFZ, Jan Mayen Fracture Zone; KR,
1246 Knipovich Ridge; ÆR, Ægir Ridge.

1247

1248 Figure 4: Tectono-stratigraphic summary for the Norwegian Sea Oceanic Basin and
1249 Prograded Margins CTSE. Chronostratigraphy based on the ICS International

1250 Chronostratigraphic Chart v2022/10 (Cohen *et al.* 2013; updated;
1251 <http://www.stratigraphy.org/ICSchart/ChronostratChart2022-10.pdf>). (1) Lithostratigraphy
1252 mid-Norwegian margin (Dalland *et al.* 1988); (2) Lithostratigraphy SW Barents Sea margin
1253 (Eidvin *et al.* 2022); (3) Seismic stratigraphy for the western Barents Sea-Svalbard margin
1254 based on Faleide *et al.* (1996) with ages updated in accordance with Knies *et al.* (2009) and
1255 Alexandropoulou *et al.* (2021). Also shown are the main hydrocarbon play elements for the
1256 CTSE. See text for more details.

1257

1258 Figure 5: Regional profiles across the Møre-Vøring margins highlighting the post-breakup
1259 succession. Profile A based on Martinsen *et al.* (1999) and Nygård *et al.* (2005). Profile B
1260 based on Gernigon *et al.* (2021) and Hjelstuen and Andreassen (2015). Profiles C-E based on
1261 Gernigon *et al.* (2021). Profile locations shown in Figs. 2, 6 and 7.

1262

1263 Figure 6: Sediment thickness maps. (A) Thickness of pre-glacial (Eocene-Pliocene)
1264 sediments (compilation based on Funck *et al.* 2017, Maystrenko *et al.* 2017, Lasabuda *et al.*
1265 2018b, Zastrozhnov *et al.* 2020, Gernigon *et al.* 2021 and Meza-Cala *et al.* 2021, in addition
1266 to in-house data). (B) Thickness of latest Pliocene-Pleistocene glacial sediments forming
1267 large trough mouth fans (TMF) deposited in front of bathymetric troughs on the Barents Sea,
1268 mid-Norwegian and northern North Sea shelves (based on Hjelstuen and Sejrup 2021). Also
1269 shown are location of profiles in Figs. 5 and 8. EGFZ, East Greenland Fracture Zone; JMFZ,
1270 Jan Mayen Fracture Zone; KR, Knipovich Ridge; LVM, Lofoten-Vesterålen Margin; NC,
1271 Norwegian Channel; ÆR, Ægir Ridge. Histogram-equalized colour scales are used in each
1272 panel for the best colour representation and visualization.

1273

1274 Fig. 7: Location of Quaternary slides along the NE Atlantic margin (Hjelstuen *et al.* 2007;
1275 Safronova *et al.* 2017). (1) BFSC II; (2) BFSC I; (3) BFSC III; (4) Slide A; (5) Slide S; (6)
1276 Bjørnøya Slide; (7) Andøya Slide; (8) Trænadjupet Slide; (9) Storegga Slide; (10)
1277 Sklinnadjupet Slide; (11) Møre Slide; (12) Tampen Slide; (13) SFU3; (14) LS-1; (15) SFU1.
1278 Also shown are CTSE outline and location of profiles in Figs. 5 and 8.

1279

1280 Figure 8: Regional profiles across the western Barents Sea-Svalbard margin highlighting the
1281 post-breakup succession. Profile A based on Faleide *et al.* (1993, 1996). Profile B based on
1282 unpublished seismic interpretation. Profile C based on Hjelstuen *et al.* (2007). Profile D

1283 based on unpublished seismic interpretation. Profile E is based Ljones *et al.* (2004). Seismic
1284 stratigraphy shown in Fig. 4. Profile locations shown in Figs. 2, 6 and 7.

1285

1286

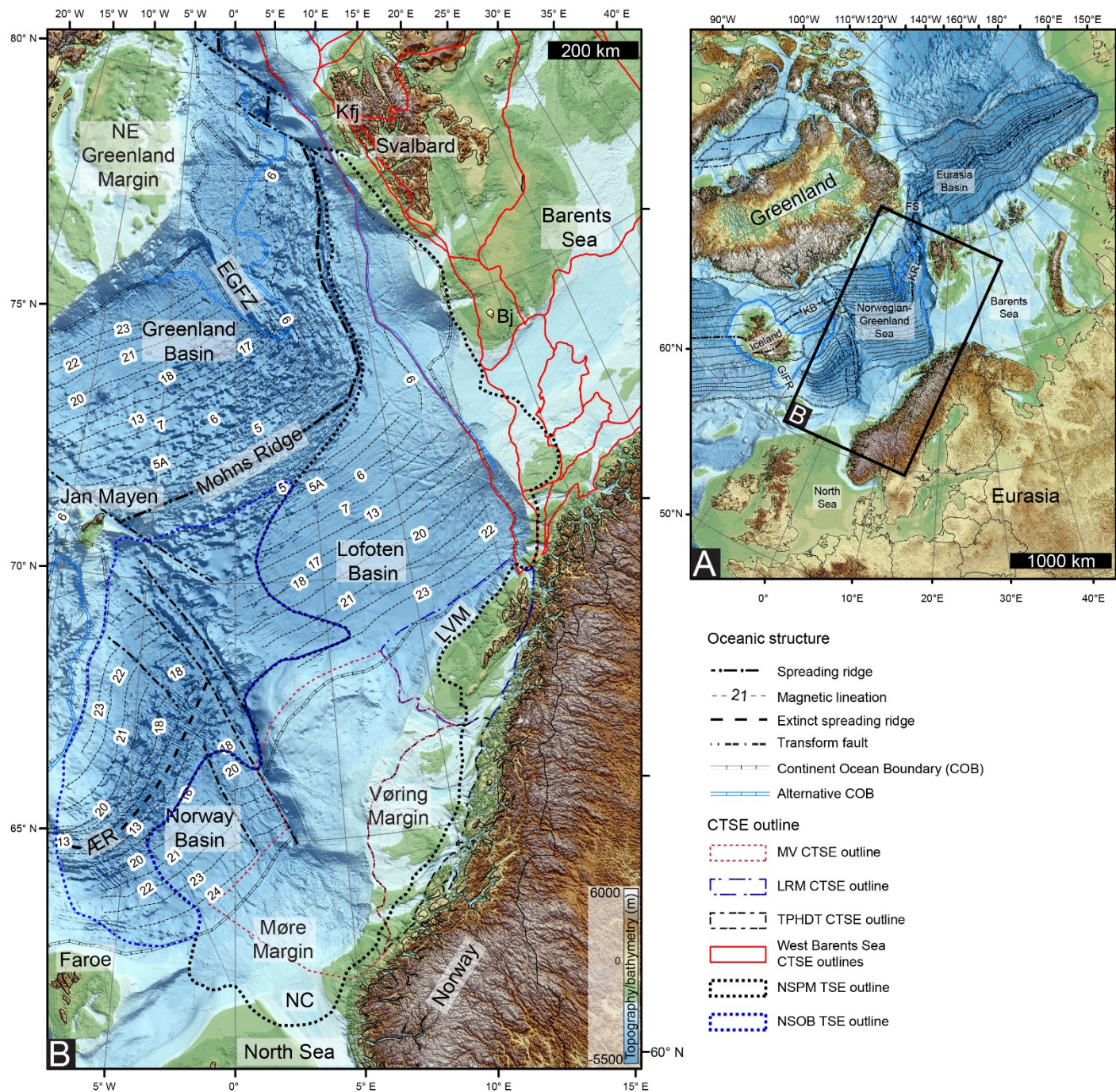


Figure 1: (A) Regional North Atlantic-Arctic setting and location of study area. (B) Study area with outline of the Norwegian Sea Oceanic Basin and Prograded Margins Composite Tectono-Sedimentary Element. Outline of other CTSE's also shown. Topography and bathymetry from IBCAO (Jakobsson *et al.* 2020) and oceanic structure based on Abdelmalak *et al.* (2023). Bj, Bjørnøya; FS, Fram Strait; EGFZ, East Greenland Fracture Zone; GIFR, Greenland-Iceland-Faroe Ridge; KB, Kolbeinsey Ridge; Kfj, Kongsfjorden; KR, Knipovich Ridge; LVM, Lofoten-Vesterålen Margin; NC, Norwegian Channel; ÆR, Ægir Ridge.

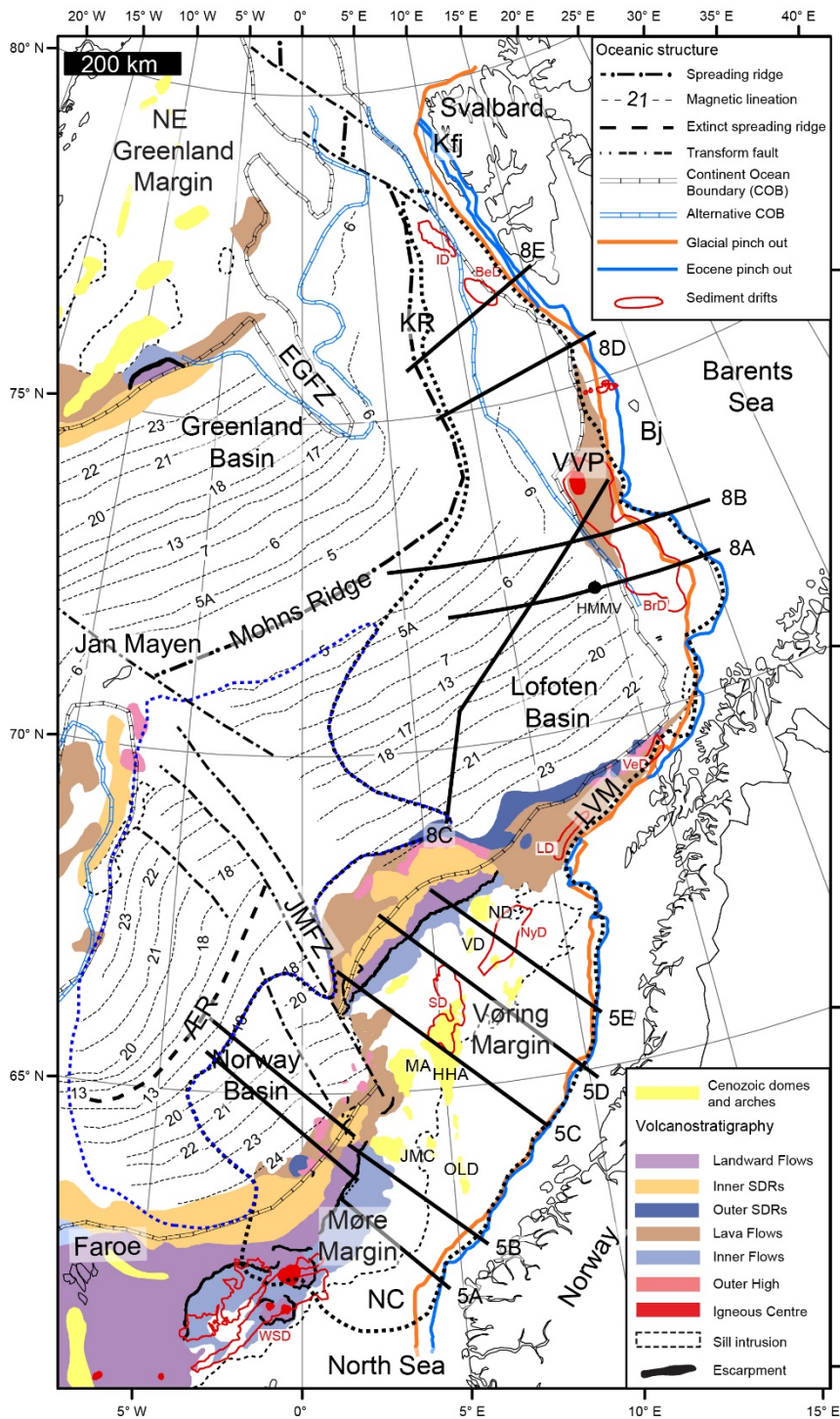


Figure 2: Breakup-related volcanics underlying the prograded margins (Gernigon et al. 2021). Outline of the Norwegian Sea Oceanic Basin and Prograded Margins CTSE. Oceanic structure based on Abdelmalak et al. (2023). Also shown are Cenozoic domes/arches (Gernigon et al. 2021), Cenozoic sediment drifts (Bjordal-Olsen 2023) and location of profiles in Figs. 5 and 8. BeD, Bellsund Drift; Bj, Bjørnøya; BrD, Bjørnøyrenna Drift; FS, EGFZ, East Greenland Fracture Zone; HHA, Helland-Hansen Arch; HMMV, Håkon Mosby Mud Volcano; ID, Isfjorden Drift; JMC, Jan Mayen Corridor; JMFZ, Jan Mayen Fracture Zone; Kfj, Kongsfjorden; KR, Knipovich Ridge; LD, Lofoten Drift; LVM, Lofoten-Vesterålen Margin; MA, Modgun Arch; ND, Naglfar Dome; NC, Norwegian Channel; NyD, Nyk Drift; OLD, Ormen Lange Dome; SD, Skinnadjuvet Drift; VD, Vema Dome; VeD, Vesterålen Drift; VVP, Vestbakken Volcanic Province; WSD, West Shetland Drift; ÆR, Ægir Ridge.

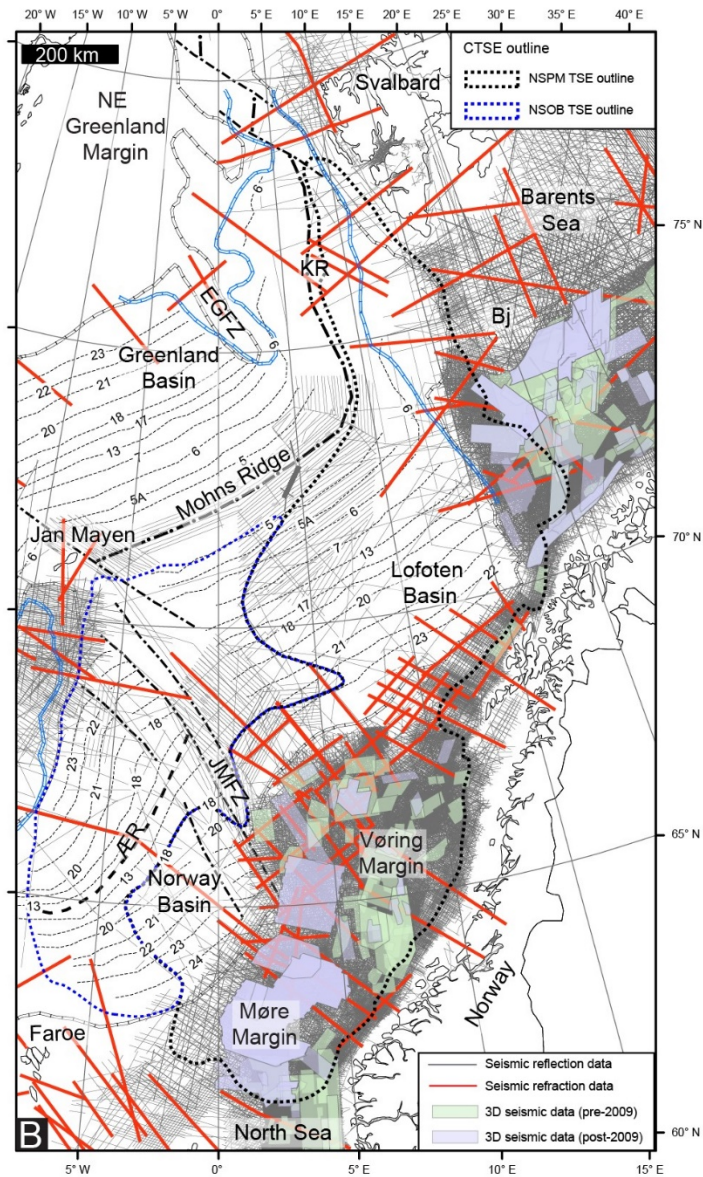
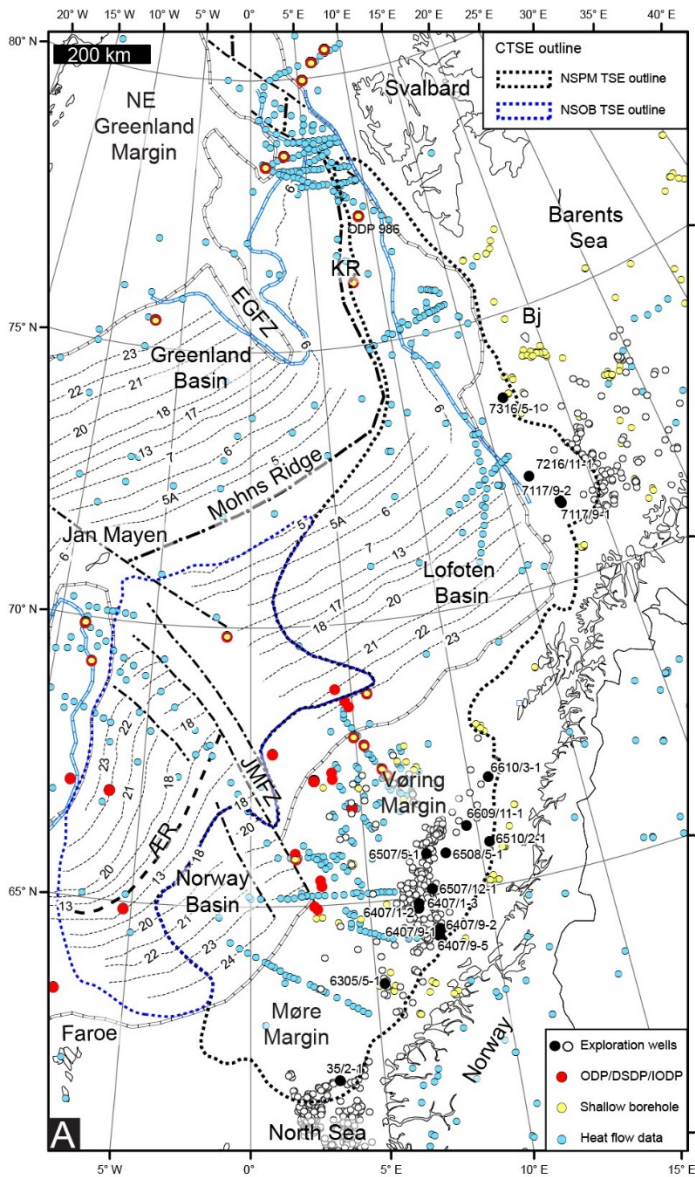


Figure 3: Data coverage. (A) Location of exploration wells and scientific/shallow stratigraphic boreholes. Key wells are highlighted and labelled. Location of heat flow measurements also shown; (B) Seismic data – regional 2D seismic reflection profiles in thin grey lines, 3D seismic cubes in colour polygons, thick red lines show deep seismic refraction data. CTSE outline shown in both maps. Oceanic structure based on Abdelmalak et al. (2023). EGFZ, East Greenland Fracture Zone; JMfZ, Jan Mayen Fracture Zone; KR, Knipovich Ridge; AER, Aegir Ridge.

Chronostratigraphy				Stratigraphy			Events	Source	Reservoir	Seal	Trap	Charge	
				(1)	(2)	(3)							
Cenozoic	Quaternary	Holocene	Ma										
		Pleistocene	Upper	~0.01	↑	↑	GIII	Slope failure - slides	Ice streams shaping the shelves	Glacial sands ?	Glacigenic debris flows ?		
			Chibanian	~0.13			R1						
			Calabrian	~0.77	Naust Fm	Naust Fm	GII						
			Gelasian	1.80			R5						
	Neogene	Pliocene	Piacenzian	2.58	↓	↓	GI	Contourite drifts	Building Trough Mouth Fans				
			Zanclean	3.60			R7						
		Miocene	Messinian	~5.3	↑	↑	G0	Onset of major glaciations and margin progradation	Onset of inner shelf progradation mid-Norway	↑			
			Tortonian	~7.25	Molo Fm								
			Serravallian	11.63	Kai Fm	Tiskjegg Fm	Te4						
			Langhian	13.82			↓						
			Burdigalian	15.97									
			Aquitanian	20.44									
			Chattian	23.03			Te3						
			Rupelian	27.82			↓						
	Paleogene	Oligocene	Chattian	27.82				Compression/inversion - domes	Fram Strait deep water connection	Injectites ?	Domes ?		
			Rupelian	33.9	Brygge Fm	Torsk Fm	Te2						
		Eocene	Priabonian	37.71				Onset of global cooling Plate reorganization	Azolla fresh water event	↓			
			Bartonian	41.2									
			Lutetian	47.8			Te1						
			Ypresian	56.0									
			PETM										
			Breakup and onset of seafloor spreading										
		Paleocene	Thanetian	59.2				Azolla fresh water event	PETM	↓			
Selandian			61.6										
Danian	66.0												

Figure 4: Tectono-stratigraphic summary for the Norwegian Sea Oceanic Basin and Prograded Margins CTSE. Chronostratigraphy based on the ICS International Chronostratigraphic Chart v2022/10 (Cohen et al. 2013; updated; <http://www.stratigraphy.org/ICSChart/ChronostratChart2022-10.pdf>). (1) Lithostratigraphy mid-Norwegian margin (Dalland et al. 1988); (2) Lithostratigraphy SW Barents Sea margin (Eidvin et al. 2022); (3) Seismic stratigraphy for the western Barents Sea-Svalbard margin based on Faleide et al. (1996) with ages updated in accordance with Knies et al. (2009) and Alexandropoulou et al. (2021). Also shown are the main hydrocarbon play elements for the CTSE. See text for more details.

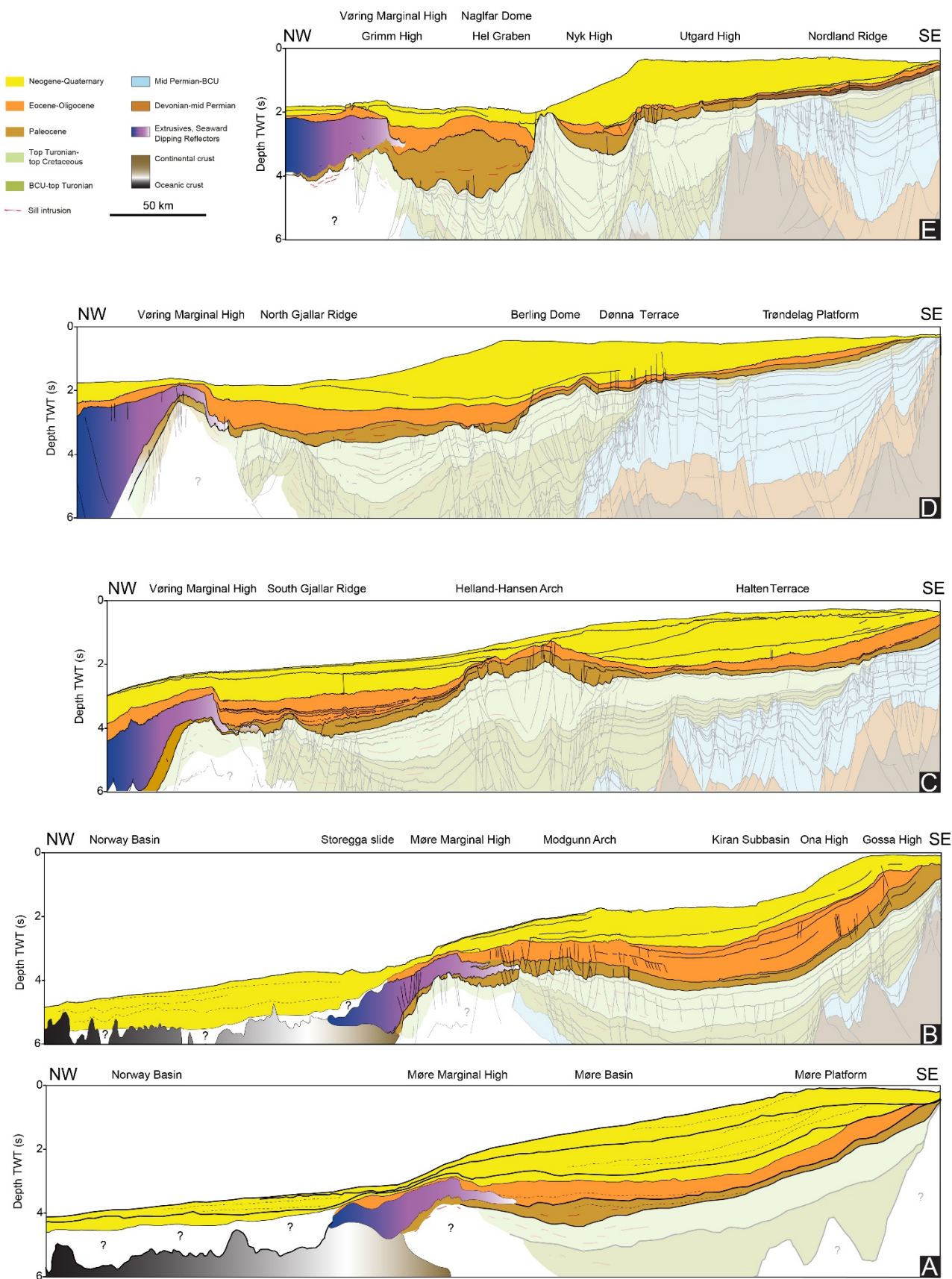


Figure 5: Regional profiles across the Møre-Vøring margins highlighting the post-breakup succession. Profile A based on Martinsen et al. (1999) and Nygård et al. (2005). Profile B based on Gernigon et al. (2021) and Hjelstuen and Andreassen (2015). Profiles C-E based on Gernigon et al. (2021). Profile locations shown in Figs. 2, 6 and 7.

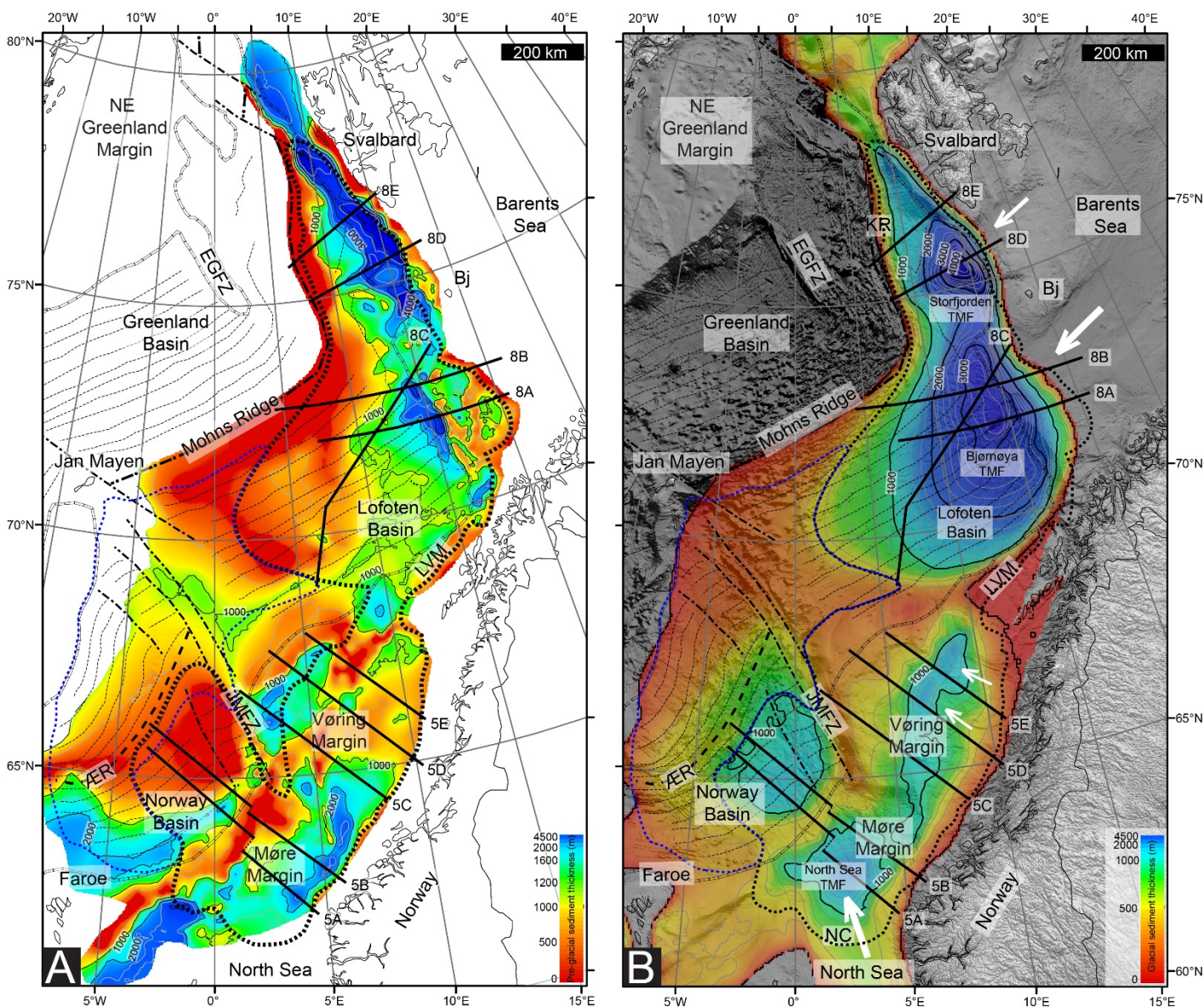


Figure 6: Sediment thickness maps. (A) Thickness of pre-glacial (Eocene-Pliocene) sediments (compilation based on Funck et al. 2017, Maystrenko et al. 2017, Lasabuda et al. 2018b, Zastrozhnov et al. 2020, Gernigon et al. 2021 and Meza-Cala et al. 2021, in addition to in-house data). (B) Thickness of latest Pliocene-Pleistocene glacial sediments forming large trough mouth fans (TMF) deposited in front of bathymetric troughs on the Barents Sea, mid-Norwegian and northern North Sea shelves (based on Hjelstuen and Sejrup 2021). Also shown are location of profiles in Figs. 5 and 8. EGFZ, East Greenland Fracture Zone; JMFZ, Jan Mayen Fracture Zone; KR, Knipovich Ridge; LVM, Lofoten-Vesterålen Margin; NC, Norwegian Channel; ÆR, Ægir Ridge. Histogram-equalized colour scales are used in each panel for the best colour representation and visualization.

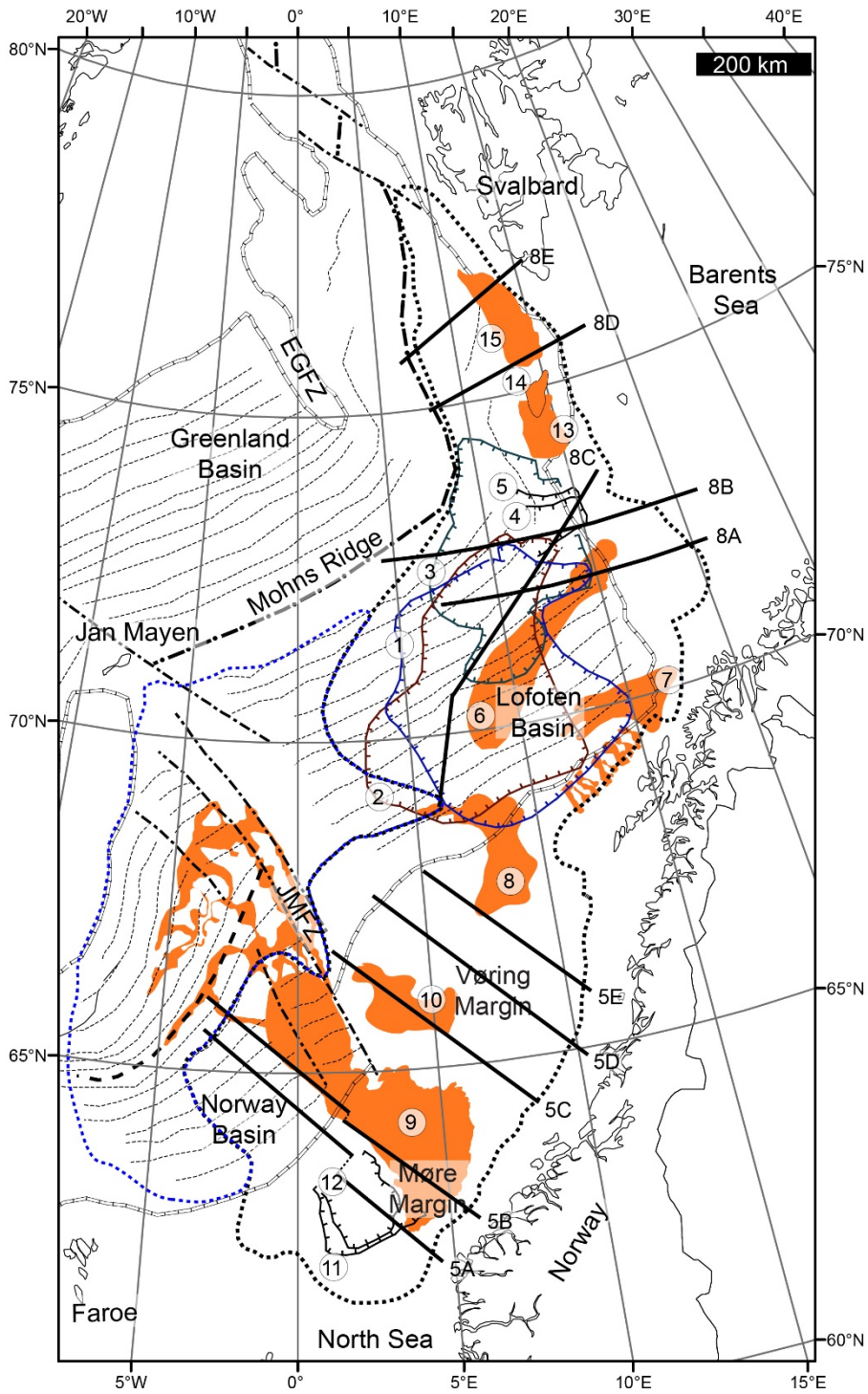


Fig. 7: Location of Quaternary slides along the NE Atlantic margin (Hjelstuen et al. 2007; Safronova et al. 2017). (1) BFSC II; (2) BFSC I; (3) BFSC III; (4) Slide A; (5) Slide S; (6) Bjørnøya Slide; (7) Andøya Slide; (8) Trænadjupet Slide; (9) Storegga Slide; (10) Sklinnadjupet Slide; (11) Møre Slide; (12) Tampen Slide; (13) SFU3; (14) LS-1; (15) SFU1. Also shown are CTSE outline and location of profiles in Figs. 5 and 8.

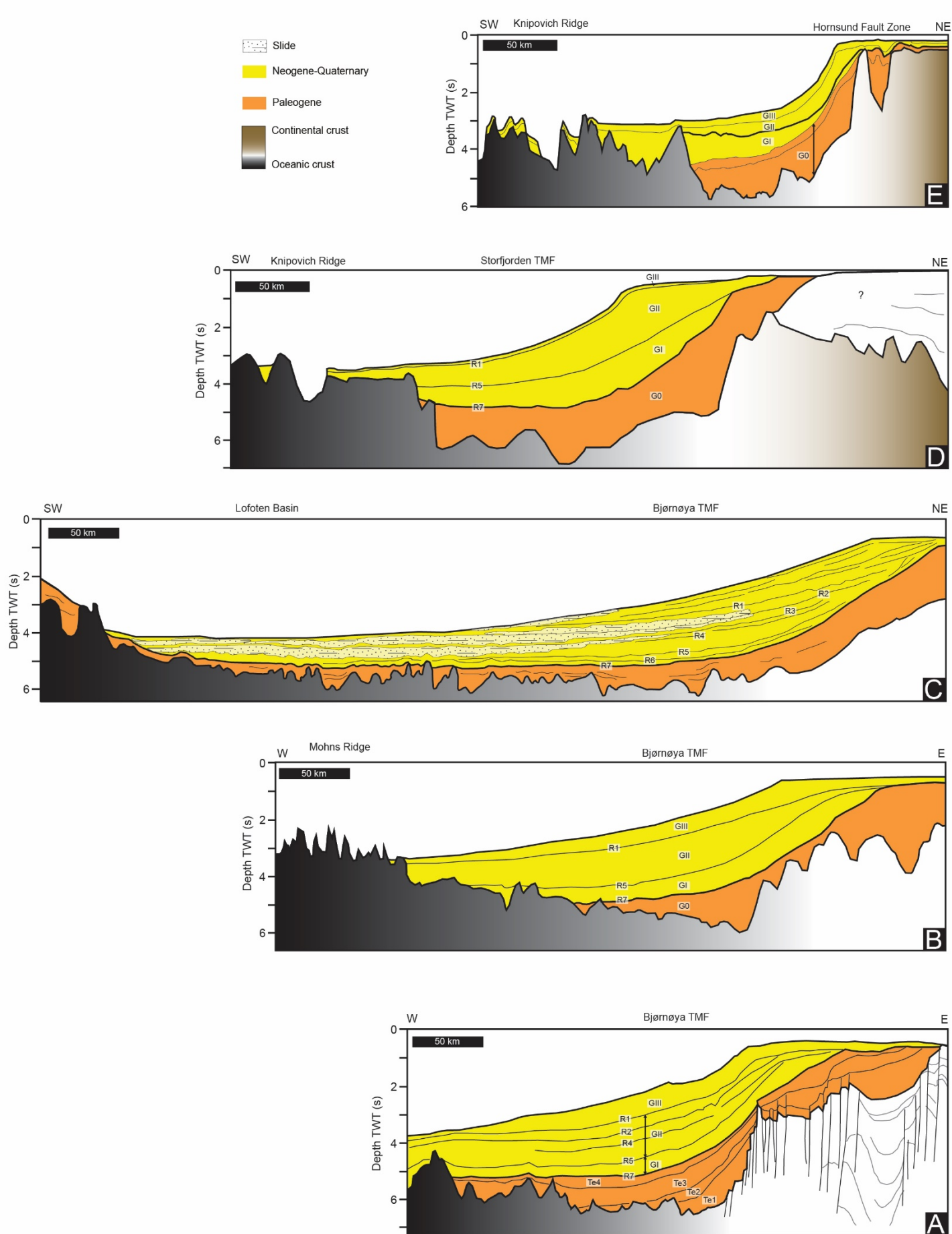


Figure 8: Regional profiles across the western Barents Sea-Svalbard margin highlighting the post-breakup succession. Profile A based on Faleide et al. (1993, 1996). Profile B based on unpublished seismic interpretation. Profile C based on Hjelstuen et al. (2007). Profile D based on unpublished seismic interpretation. Profile E is based Ljones et al. (2004). Seismic stratigraphy shown in Fig. 4. Profile locations shown in Figs. 2, 6 and 7.